THE GEOLOGICAL SOCIETY OF AMERICA®

The Ediacaran–Cambrian transition in the southern Great Basin, United States

Emily F. Smith[1,†], Lyle L. Nelson[1,3], Nizhoni O'Connell[2], Athena Eyster[1], and Mary C. Lonsdale[1]
[1]*Department of Earth and Planetary Sciences, Johns Hopkins University, 3400 North Charles Street, Olin Hall, Baltimore, Maryland 21218, USA*
[2]*Department of Earth and Planetary Sciences, Harvard University, 20 Oxford Street, Cambridge, Massachusetts 02138, USA*
[3]*Department of Earth Sciences, Carleton University, 1125 Colonel By Drive, Ottawa, Ontario K1S 5B6, Canada*

ABSTRACT

The Ediacaran–Cambrian boundary strata in the Great Basin of the southwestern United States record biological, geochemical, and tectonic change during the transformative interval of Earth history in which metazoans diversified. Here, we integrate new and compiled chemostratigraphic, paleontological, sedimentological, and stratigraphic data sets from the Death Valley region, the White-Inyo Ranges, and Esmeralda County in Nevada and California and evaluate these data within a regional geologic framework. A large negative carbon isotope ($\delta^{13}C$) excursion—also known as the Basal Cambrian Excursion, or BACE—is regionally reproducible, despite lateral changes in sedimentary facies and dolomitization across ~250 km, consistent with a primary marine origin for this perturbation. Across the southern Great Basin, Ediacaran body fossils are preserved in a variety of taphonomic modes, including cast and mold preservation, two-dimensional compressional preservation, two-dimensional and three-dimensional pyritization, and calcification. The stratigraphic framework of these occurrences is used to consider the relationships among taphonomic modes for fossil preservation and paleoenvironmental settings within this basin. In this region, Ediacaran-type fossils occur below the nadir of the BACE, while Cambrian-type trace fossils occur above. Sedimentological features that include giant ooids, stromatolites, and textured organic surfaces are widespread and abundant within the interval that records biotic turnover and coincide with basaltic volcanism and the BACE. We hypothesize that the prevalence of these sedimentological features, the BACE, and the disappearance of some Ediacaran clades were caused by environmental perturbation at the Ediacaran–Cambrian boundary.

INTRODUCTION

The Great Basin of southwestern North America hosts iconic Neoproterozoic and Cambrian strata that have captured the attention, imagination, and admiration of geologists and enthusiasts of the natural world. The Cryogenian Kingston Peak Formation includes an extensive sedimentological record of glaciation with some of the most accessible and well-exposed snowball Earth glacial deposits in North America (e.g., Prave, 1999). The overlying dolostone of the basal Ediacaran Noonday Formation contains sedimentary features such as tubestone stromatolites and giant wave ripples that are characteristic of Marinoan cap carbonates globally (e.g., Corsetti and Grotzinger, 2005; Petterson et al., 2011). The Ediacaran Johnnie Formation includes the Rainstorm Member, which is known for unusual sedimentological features such as aragonite fans (e.g., Pruss et al., 2008) and a laterally extensive oolite, and for its record of the Shuram carbon isotope ($\delta^{13}C$) excursion, the largest negative carbon isotope excursion in Earth history (e.g., Kaufman et al., 2007). Overlying the Johnnie Formation are units recording the Ediacaran–Cambrian transition—the Stirling Quartzite and Wood Canyon Formation—as well as their more distal equivalents exposed to the northwest in the White-Inyo Ranges—the Reed Dolomite and the Deep Spring Formation. These units host rare, but in some cases, well-preserved, soft-bodied Ediacaran fossils (e.g., Horodyski, 1991; Hagadorn and Waggoner, 2000; Smith et al., 2016b, 2017). The southern Great Basin was one of the first regions where the first occurrence of the trace fossil *Treptichnus pedum*, the formal marker of the base of the Cambrian, was stratigraphically linked to a large negative $\delta^{13}C$ excursion (Corsetti and Hagadorn, 2000), which is now a secondary stratigraphic marker used to identify the Ediacaran–Cambrian boundary in many localities globally. In addition, these units have been interpreted as recording the final stages of rifting in southwestern Laurentia before the establishment of the Paleozoic passive margin (e.g., Bond et al., 1985). These strata are important archives for understanding potential links among biotic change, environmental perturbations, and tectonism across the Ediacaran–Cambrian boundary.

Formal geologic studies on the Neoproterozoic and Cambrian strata began in the late nineteenth century (e.g., Gilbert, 1875; Turner, 1902; Spurr, 1903; Ball, 1907). Edwin Kirk, a U.S. Geological Survey (USGS) scientist, provided the first systematic and detailed study of Ediacaran and Cambrian strata of the region, naming many of the units in the Inyo Range in a USGS professional paper (Knopf, 1918). Shortly thereafter, Thomas Nolan mapped the Spring Mountains of Nevada and formalized many of the equivalent Ediacaran–Cambrian units of the Death Valley region—names that are still in use today—as part of his Ph.D. dissertation (Nolan, 1924, 1929). In the decades that followed, many important geological contributions, including geologic mapping and stratigraphic, petrographic, and paleontological studies, continued to increase understanding of the Ediacaran–Cambrian stratigraphy of the southern Great Basin. Of particular note, Wheeler (1948) was the first to propose stratigraphic correlations of Neoproterozoic and Cambrian units across a large area of the Great Basin, and several others have since built off of this early regional framework. The seminal works by USGS scientist John (Jack) Stewart (e.g., Stewart, 1965, 1967, 1970, 1983; Stewart et al., 1968) contributed detailed sedimentologic observations and an exhaustive regional stratigraphic framework for Neoproterozoic–Cambrian units of southwestern North America that continue to provide a robust foundation for the geologic studies of these strata.

Emily F. Smith https://orcid.org/0000-0001-9260-9355
†efsmith@jhu.edu.

GSA Bulletin; May/June 2023; v. 135; no. 5/6; p. 1393–1414; https://doi.org/10.1130/B36401.1; 11 figures; 1 supplemental file.
published online 22 September 2022

Since Jack Stewart published his comprehensive USGS professional paper of the southern Great Basin (Stewart, 1970), there have been a number of regional studies, the development and application of new analytical techniques, and an improved understanding of the Ediacaran–Cambrian transition regionally and globally. Some of these advancements include: (1) the development of carbon isotope chemostratigraphy (e.g., Shackleton and Hall, 1984; Berner, 1990; Kump and Arthur, 1999) and application of this tool to Neoproterozoic–Cambrian units in the southwestern USA (Corsetti and Kaufman, 1994; Prave, 1999; Abolins et al., 2000; Corsetti and Hagadorn, 2000); (2) new techniques for U-Pb radioisotopic dating (e.g., Krogh, 1973; Mattinson, 2005) and radioisotopic ages that led to an improved temporal framework for Neoproterozoic and Cambrian units in southwestern North America and globally (e.g., Mahon et al., 2014; Rooney et al., 2018; Karlstrom et al., 2018, 2020; Nelson et al., 2020, 2022; Hodgin et al., 2021); and (3) fossil discoveries in the Great Basin that allow for improved paleontological integration of this region with other Ediacaran–Cambrian sites globally (Corsetti and Hagadorn, 2000; Hagadorn and Waggoner, 2000; Jensen et al., 2002; Smith et al., 2016b, 2017; Selly et al., 2020). The aim of this paper is to provide a comprehensive, regional perspective on the geology of the Ediacaran–Cambrian transition in the Great Basin that integrates decades of observations and data with new, high-resolution carbon isotope and paleontological data into an updated stratigraphic, paleoenvironmental, and tectonic framework.

GEOLOGIC BACKGROUND

Neoproterozoic to early Cambrian strata in the Great Basin of southwestern North America were deposited during episodic rifting associated with the breakup of Rodinia prior to the development of a passive margin along the length of the Cordilleran margin in the Cambrian (Stewart, 1970; Armin and Mayer, 1983; Bond and Kominz, 1984; Bond et al., 1985; Levy and Christie-Blick, 1991; Fedo and Cooper, 2001). Ediacaran–Cambrian basin architecture in the Great Basin manifests as stratigraphic thickening from southeast to northwest, with siliciclastic-dominated successions in the Death Valley region deposited in fluvial deltaic to proximal shelf environments, and thicker, more carbonate-dominated successions in the White-Inyo Ranges and Esmeralda County deposited in shelf to outer shelf environments referred to here as the "Inyo facies" (Fig. 1) (Stewart, 1970; Nelson, 1976; Nelson, 1978; Fedo and Cooper, 1990; Mount et al., 1991; Corsetti and Hagadorn, 2000; Fedo and Cooper, 2001). As such, these two regions—the Death Valley region and the ranges to the north–northwest—use different stratigraphic nomenclature. In addition, the Death Valley region hosts kilometers of early Ediacaran and pre-Ediacaran strata that are not exposed farther to the northwest.

Precise regional correlations and depositional basin reconstructions of Ediacaran units have been hindered by a lack of exposure in the transitional area between the two regions and a complex deformational history, which spans from the late Paleozoic to the late Cenozoic. Contractional deformation in the White-Inyo Ranges occurred before the emplacement of mid- to late Mesozoic plutons as indicated by plutons younger than ca. 180 Ma that truncate folds and faults (Dunne et al., 1978; Morgan and Law, 1998; Coleman et al., 2003). The Last Chance thrust fault (Fig. 1) is particularly relevant to this study, as it is an east- to southeast-vergent structure that is thought to have juxtaposed outer shelf Inyo strata in the northwest against the inner shelf Death Valley strata in the southeast between the late Early Permian and middle Early Triassic (either the Antler or Sonoma Orogen) (Stewart et al., 1966; Stevens and Stone, 2005). All of the Inyo facies strata are thought to overlie this thrust fault with shortening of $\sim$30 km (Stewart et al., 1966). The areas included in this study were also deformed by northeast–southwest-trending contractional Jurassic–Cretaceous structures that are related to the Sevier Orogeny (Burchfiel and Davis, 1972; DeCelles, 2004). Subsequent Cenozoic extension and strike-slip deformation in the region led to tilting and exhumation and was also accompanied by felsic and mafic igneous intrusions and volcanism (Wernicke et al., 1988; Snow et al., 1991; Snow and Wernicke, 2000; Stockli et al., 2003; Pavlis et al., 2014). Despite structural complexities, the Death Valley and the White-Inyo strata have been correlated using lithostratigraphy, sequence stratigraphy, chemostratigraphy, and biostratigraphy (Fig. 2) (Stewart, 1970; Corsetti and Hagadorn, 2000, 2003).

In the Death Valley region, Mesoproterozoic to Cryogenian sedimentary strata of the Pahrump Group are overlain by the Noonday Formation, which has been identified as a basal Ediacaran Marinoan cap carbonate based on lithostratigraphy, chemostratigraphy, and geochronology (Prave, 1999; Petterson et al., 2011; Nelson et al., 2020). The Johnnie Formation overlies the Noonday Formation, is $<$1500 m thick, and contains fluvio-deltaic siliciclastic rocks at its base that are overlain by marginal marine mixed siliciclastic and carbonate rocks (Stewart, 1970; Summa, 1993; Verdel et al., 2011). At the base of the Rainstorm Member, the youngest member of the Johnnie Formation, is a distinctive tan to orange oolitic dolostone ("the Johnnie Oolite"), which is overlain by mixed siliciclastic and carbonate rocks containing distinctive aragonite seafloor fans (Pruss et al., 2008). Carbonate rocks of the Rainstorm Member preserve a large negative $\delta^{13}C$ excursion, with values as low as $-12‰$, that has been correlated to the Shuram-Wonoka carbon isotope excursion (e.g., Burns and Matter, 1993; Corsetti and Kaufman, 2003; Halverson et al., 2005; Verdel et al., 2011) and marks a perturbation to global oceans between 574.0 ± 4.7 Ma and 567.3 ± 3.0 Ma (Rooney et al., 2020). No fossils have been reported from the Johnnie Formation.

The contact between the Johnnie Formation and the overlying Stirling Quartzite has been interpreted as an erosional unconformity with evidence of valley incision (e.g., Stewart, 1970; Christie-Blick and Levy, 1989; Summa, 1993; Clapham and Corsetti, 2005). This incision has been variably related to syn-depositional faulting and to eustatic sea-level fluctuations (Summa, 1993; Levy et al., 1994; Abolins et al., 2000; Clapham and Corsetti, 2005; Witkosky and Wernicke, 2018). Recently published radioisotopic ages constraining the Gaskiers glaciation (Pu et al., 2016) and the Shuram carbon isotope excursion (Rooney et al., 2020) suggest that the basal Stirling incision is too young to be driven by eustatic sea-level changes related to the Gaskiers, as it overlies the Shuram-correlative Rainstorm Member. The Stirling Quartzite (Nolan, 1929) is composed primarily of quartz arenite, which ranges from sandstone to pebble conglomerate, but also contains lesser siltstone and carbonate, particularly in more northern and western sections (Stewart, 1970). This unit has been informally subdivided into five regional members labeled A through E (Fig. 2; Stewart, 1966; Wertz, 1982). The lower and upper parts of the Stirling Quartzite (members A–B and E, respectively) are light-colored quartz sandstone and conglomerate. Member C is the recessive middle part of the formation and composed predominantly of gray to purple micaceous siltstone. Member D is most well-developed in the northwestern sections, where it is composed of predominately sucrosic and recrystallized carbonate grainstone (Fig. 2). Overall, the Stirling Quartzite has been interpreted to reflect change from a high-energy depositional environment to a lower energy one, then back to a high-energy environment in the upper part of the unit, all within distal braid plain to shallow marine depositional settings (Wertz, 1982; Fedo and Cooper, 2001).

In the White-Inyo Ranges (eastern California) and Esmeralda County (Nevada), the oldest exposed rocks are sedimentary strata of the

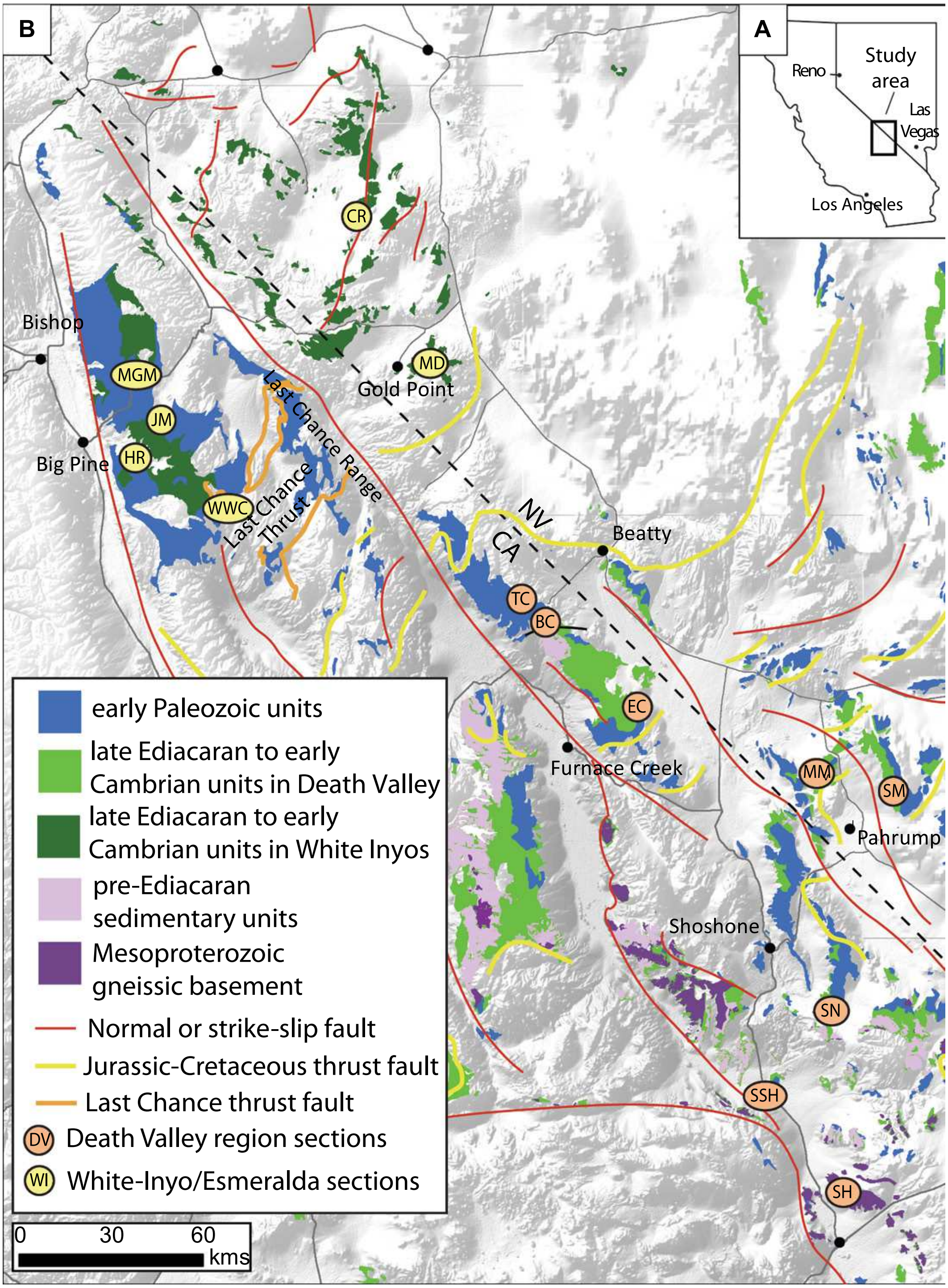

Figure 1. (A) Locality map shows study area in eastern California and western Nevada. (B) Map shows the distribution of Mesoproterozoic basement, pre-Ediacaran sedimentary units, Ediacaran to early Cambrian units (focus of this study), and early Paleozoic units across California and Nevada. Geologic map is adapted from Ludington et al. (2007), Renik and Christie-Blick (2013), and Giallorenzo et al. (2018). Last Chance thrust fault is adapted from Stewart et al. (1966) and Stevens and Stone (2005). Abbreviations for measured sections: BC—Boundary Canyon; CR—Clayton Ridge; EC—north of Echo Canyon; HR—Hines Ridge; JM—Juniper Mountain; MD—Mt. Dunfee; MGM—Molly Gibson Mine; SH—Silurian Hills; SN—Southern Nopahs; MM—Montgomery Mountains; SM—Spring Mountains; SSH—Salt Spring Hills; TC—Titanothere Canyon; WWC—Whippoorwill Canyon. CA—California; NV—Nevada.

Ediacaran Wyman Formation, which are estimated to be >1500 m thick (Nelson, 1962). The thickest continuous sections in Esmeralda County are ~400 m (Stewart, 1970). The Wyman Formation is composed dominantly of fine-grained siliciclastic strata with interbeds of limestone to sandy limestone (<15 m thick), which are commonly oolitic and locally dolomitized. Overlying the Wyman Formation is the Reed Dolomite. In the White-Inyo Ranges, an erosional unconformity has been locally documented at this contact (Nelson, 1962; Lorentz, 2007); however, at localities in Esmeralda County, the contact has been interpreted as gradational (Albers and Stewart, 1972). The Reed Dolomite is ~500 m thick, predominantly composed of massive dolostone, and locally contains beds of stromatolites, ooids, pisoids, and oncoids (Fig. 2; Stewart, 1970). The Hines Tongue is a laterally variable wedge of siliciclastic strata that occurs within the Reed Dolomite and ranges from 0 m to 240 m in thickness between the lower and upper carbonate members (Nelson, 1962). The upper member of the Reed Dolomite contains the late Ediacaran fossil *Cloudina* (Fig. 2; Taylor, 1966; Gevirtzman and Mount, 1986; Grant, 1990).

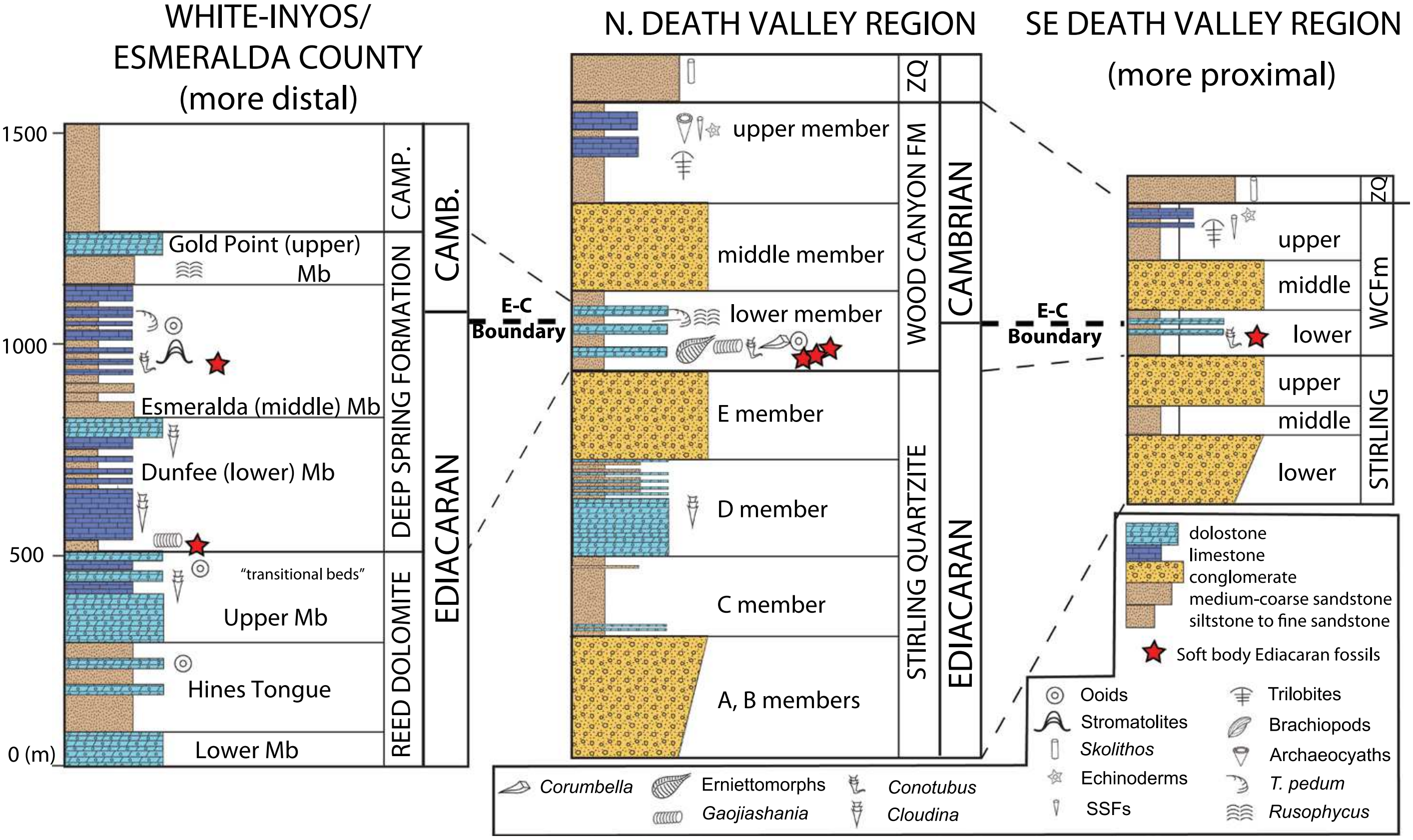

Figure 2. Generalized stratigraphy, proposed correlations, and Ediacaran–Cambrian biostratigraphy for the Death Valley Region and the White-Inyo/Esmeralda County Region are shown. Red stars indicate the stratigraphic locations of soft-bodied Ediacaran fossils. Mb—member; ZQ—Zabriskie Quartzite; Camp.—Campito Formation; E–C—Ediacaran–Cambrian; SSF—small shelly fossils; WC—Wood Canyon Formation.

Detailed sedimentological, stratigraphic, and biostratigraphic descriptions of the strata containing the Ediacaran–Cambrian boundary in both regions, as well as correlations between the regions, are described in the sections that follow.

METHODS

Fieldwork on Ediacaran through Cambrian units in California and Nevada was conducted during multiple field seasons between 2014 and 2019. Twenty-four localities were visited as part of this study. At 14 of these sites, sections were measured, and the results presented here focus on stratigraphic data from the lower member of the Wood Canyon Formation in the broader Death Valley region and the upper Reed Dolomite and the Deep Spring Formation in the White-Inyo Ranges and Esmeralda County. At some of the localities, the strata were measured as composite sections in the field to avoid measuring across faults. Chemostratigraphic and paleontological samples were collected while stratigraphic sections were logged. The transgressive-regressive sequence approach is the sequence stratigraphic approach applied to these sections (Johnson and Murphy, 1984; Catuneanu, 2019). Descriptions and detailed information for each locality visited, including sites where stratigraphic sections were not measured, can be found in the Supplemental Material[1].

Carbonate samples were collected at 0.2–2.0 m resolution where exposed. Samples were cut and micro-drilled at Harvard University and Johns Hopkins University. Samples were micro-drilled along individual laminations, where visible, to obtain 5–20 mg of carbonate powder; veins, fractures, and siliciclastic-rich laminae were avoided. In total, carbon ($\delta^{13}C$) and oxygen ($\delta^{18}O$) isotopic measurements were obtained on 1292 carbonate samples, and these are collated with previously published data from Smith et al. (2016b, 2017). Between 2014 and 2016, $\delta^{13}C$ and $\delta^{18}O$ of the carbonates were analyzed at the Harvard University Laboratory for Geochemical Oceanography, and between 2017 and 2018, they were analyzed in the Stable Isotope Geochemistry Lab at Washington University, St. Louis, Missouri, USA. Samples collected in 2019 were analyzed in the Johns Hopkins Stable Isotope Lab.

At Harvard, carbonate $\delta^{13}C$ and $\delta^{18}O$ data were acquired simultaneously on a VG Optima dual inlet mass spectrometer. Carbonate samples were reacted with orthophosphoric acid using a VG Isocarb preparation device, which includes a common acid bath with a magnetic stirrer. Approximately 1 mg of each sample was reacted in the bath at 90 °C. Evolved CO_2 was collected cryogenically and analyzed using an in-house reference gas. Reaction times for dolomite samples were increased to ~7 min to minimize potential memory effects resulting from partially unreacted samples in the common acid-bath system. Memory effect is estimated at 0.1 per mil (‰) based on the variability of standards run after dolomite samples.

[1]Supplemental Material. Carbon and oxygen isotopic data and descriptions of and GPS coordinates for key localities. Please visit https://doi.org/10.1130/GSAB.S.20387352 to access the supplemental material, and contact editing@geosociety.org with any questions.

In the Stable Isotope Geochemistry Lab at Washington University, carbonate samples for isotopic analyses were prepared by dissolving ~100 μg in 100% phosphoric acid (H_3PO_4) for at least 4 h at 70 °C. Sample vials were subsequently flushed with He, and the evolved CO_2 was measured on a Thermo Finnigan Gasbench II coupled to a Delta V Advantage isotope ratio mass spectrometer (IRMS). Carbon and oxygen isotopes are expressed in standard δ notation ($\delta^{13}C$, $\delta^{18}O$) in ‰ as a deviation from the Vienna Pee Dee Belemnite (VPDB) standard by calibration against NBS 19, NBS 20, and two in-house standards. From standard and replicate measurements, the 1σ error on $\delta^{13}C$ is <0.15‰ and on $\delta^{18}O$ is <0.2‰.

In the Johns Hopkins IRMS Laboratory, samples were analyzed for carbon and oxygen isotopic compositions using a GasBench II peripheral device coupled to a Thermo-Finnigan MAT253 IRMS in continuous-flow mode. Approximately 0.3 mg of carbonate powder reacted with 100% phosphoric acid in helium-purged vials at 30 °C overnight. Evolved CO_2 gas was then analyzed against tank CO_2 gas, and isotopic results were normalized to VPDB per mil (‰) scale using working, in-house carbonate standards (ICM, Carrara Marble, and IVA Analysentechnik, calcium carbonate) that are calibrated against international standards NBS-18 and IAEA-603. A standard deviation of 1σ of $\delta^{13}C$ and $\delta^{18}O$ values for in-house standards was <0.02‰ and <0.14‰, respectively.

Carbon and oxygen chemostratigraphic data from the Mt. Dunfee and the north of Echo Canyon sections were published in Smith et al. (2016b) and Smith et al. (2017), respectively, and the data can be found in the supplemental materials of these publications. All other chemostratigraphic data included here can be found in the Supplemental Material (see footnote 1).

STRATIGRAPHY OF THE EDIACARAN–CAMBRIAN TRANSITION IN THE SOUTHWESTERN USA

Age Control on Ediacaran–Cambrian Boundary Strata in the Southern Great Basin

No magmatic radioisotopic ages currently exist for Ediacaran to early Cambrian strata in California or Nevada. There are U-Pb detrital zircon maximum depositional ages of 527 ± 12 Ma from the Campito Formation in California (Chapman et al., 2015) and 507.68 ± 0.36 Ma from the Tapeats Sandstone at Frenchman Mountain in Nevada (Karlstrom et al., 2020). Thus, age models for the Ediacaran–Cambrian strata in the Death Valley, White-Inyo Ranges, and Esmeralda County primarily have been developed using biostratigraphy (Hagadorn and Bottjer, 1997; Hagadorn and Waggoner, 2000), chemostratigraphy (Corsetti and Hagadorn, 2000; Corsetti and Kaufman, 2003), and correlations to other radioisotopically constrained sections. The youngest reported zircon grains from the La Ciénega Formation, in Sonora, Mexico, have yielded a weighted mean $^{206}Pb/^{238}U$ date of 539.40 ± 0.23 Ma using chemical abrasion isotope dilution-thermal ionization mass spectrometry (CA-ID-TIMS), which is suggested to be a near-depositional age (Hodgin et al., 2021). This date is from a bed ~20 m above carbonate strata recording the nadir of a large negative carbon isotope ($\delta^{13}C$) excursion that has been correlated to a negative $\delta^{13}C$ excursion of similar magnitude in the lower member of the Wood Canyon Formation and the Dunfee Member of the Deep Spring Formation, and globally to the basal Cambrian carbon isotope excursion (BACE) (Loyd et al., 2012).

Ediacaran–Cambrian Boundary Strata in the Death Valley Region

In the Death Valley region, the Ediacaran–Cambrian transition is recorded in the lower member of the Wood Canyon Formation (Fig. 2). All of the sections included in this study are north of Baker, California, and thus considered "off craton" settings, with the northeast–southwest-trending craton margin hinge zone interpreted to be ~50 km to the SE of Baker (Hogan et al., 2011). In the more distal off craton settings, the lower member of the Wood Canyon Formation contains three parasequences, each of which is capped by a tan dolostone marker bed (Fig. 3A; Stewart, 1970; Diehl, 1974; Fedo and Prave, 1991). In most sections, the dolostone marker beds are coarsely recrystallized, but there are some localities in which original sedimentological features are discernible. In at least two localities (Titanothere Canyon and the Montgomery Mountains), ooids and/or pisoids (>2 mm) are present in all three of the dolostone marker beds and mainly preserved as ooid ghosts (Fig. 4D). Pisoids or "giant ooids" were only found in the lowest marker bed. North of Echo Canyon, small, <6 cm tall stromatolites occur in the lowest marker bed (Fig. 4C). Apart from the thin intervals of dolostone, the remainder of the unit is composed of micaceous siltstone to medium-grained sandstone with minor shale and coarse-grained, quartz-rich sandstone channels. Microbially mediated sedimentary structures in siltstone and sandstone are commonly present on bedding plane exposures of fine-grained siliciclastic facies (Fig. 4B; Hagadorn and Bottjer, 1999); with the exception of the newly reported stromatolites from the section north of Echo Canyon, no stromatolites or other microbial structures have been reported from carbonate beds in the lower member of the Wood Canyon Formation. The depositional environment of this member has been interpreted as the distal edge of a braid-delta, in which marine facies interfinger with fluvial sands (Fedo and Cooper, 2001). The base of the overlying middle member of the Wood Canyon Formation, a unit of coarse sandstone to conglomerate that records a fluvially dominated braidplain environment, is interpreted as an angular unconformity based on regional truncation of the lower member (Diehl, 1979; Fedo and Prave, 1991).

A number of biostratigraphically significant fossils occur in the Ediacaran strata of the Death Valley region. The calcified Ediacaran fossil *Cloudina* was reported from carbonate beds in the informal member D of the Stirling Quartzite in the Funeral Mountains (Langille, 1974)—although these are figured in low-resolution and remain to be reidentified. In the overlying lower member of the Wood Canyon Formation, Ediacaran body fossils below the lowest dolostone marker bed were reported from the Montgomery Mountains, including casts and molds and two-dimensional forms of tubular fossils including *Gaojiashania*, problematic discoidal fossils, and additional tubular body fossils preserved as two- and three-dimensional iron oxides, including *Conotubus*, *Corumbella*, and *Gaojiashania* (Hagadorn and Waggoner, 2000; Smith et al., 2017). In a subsequent taxonomic study of the tubular fossils from this interval, specimens originally interpreted as *Conotubus* were reassigned to two distinct taxa of cloudinids: *Saarina hagadorni* and *Costatubus bibendi* (Selly et al., 2020). Tomographic analyses of some of these iron oxide-replaced cloudinomorph fossils showed internal tubular structures, which were interpreted as formerly pyritized soft tissue that may have been bilaterian digestive tracts (Schiffbauer et al., 2020).

Fossils assigned to *Ernietta* and *Swartpuntia*, belonging to one of the classic morphoclades of Ediacaran Biota, erniettomorphs, were reported from the lower member of the Wood Canyon Formation in the Montgomery Mountains (Horodyski, 1991; Hagadorn and Waggoner, 2000; Smith et al., 2017; Runnegar, 2021). Additionally, one fragment of a frond-like, soft-bodied fossil was reported from the upper member of the Wood Canyon Formation in the Kelso Mountains, California, and was tentatively assigned to the Ediacaran erniettomorph *Swartpuntia* (Hagadorn et al., 2000).

In the Death Valley region, the first recognized occurrence of the basal Cambrian index trace fossil *Treptichnus pedum (T. pedum)* is located

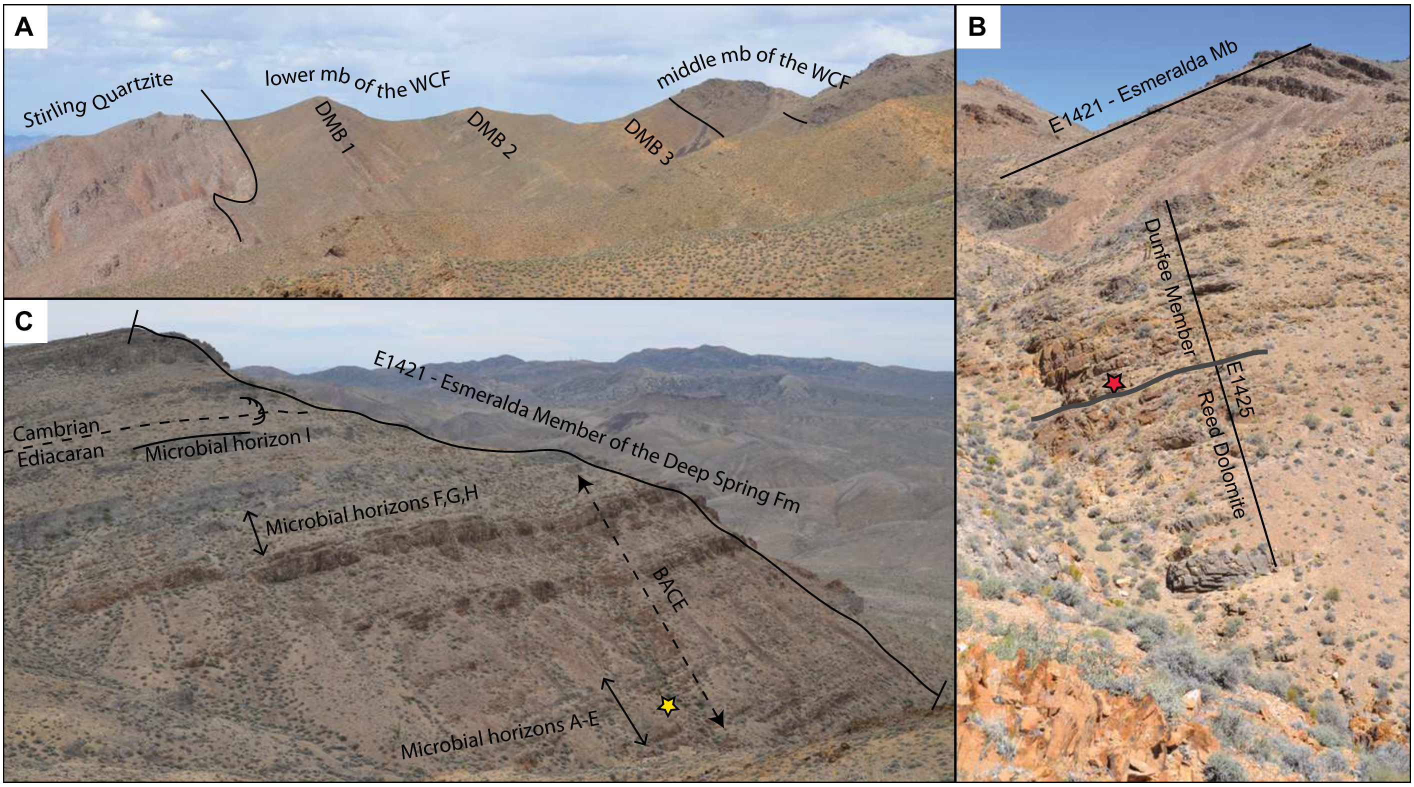

Figure 3. Field photographs show late Ediacaran–Cambrian transition strata in the southern Great Basin. (A) Section of the upper Stirling Quartzite through the lower part of the middle member (mb) of the Wood Canyon Formation (WCF) in Montgomery Mountains. DMB—Dolomite marker bed. (B) A fault block of the Dunfee (lower) Member of the Deep Spring Formation at Mt. Dunfee, Nevada, with a separate fault block of the Esmeralda Member behind it. Section numbers E1421 and E1425 refer to sections published in Smith et al. (2016b). The red star marks the Dunfee Member fossil horizon. (C) Photo of the Esmeralda (middle) Member of the Deep Spring Formation at Mt. Dunfee, Nevada. The yellow star marks the pyritized cloudinid horizon from Smith et al. (2016b) and Selly et al. (2020). Lettered microbial horizons correspond to those in Rowland et al. (2008).

just above the second dolostone marker of the lower member of the Wood Canyon Formation (Corsetti and Hagadorn, 2000). Because the basal Cambrian Global Boundary Stratotype Section and Point (GSSP) in Newfoundland was intended to coincide with the FAD of *T. pedum* (Narbonne et al., 1987), the Ediacaran–Cambrian boundary in the Death Valley region was placed at this stratigraphic horizon. The underlying dolostone bed contains the nadir of a negative δ^{13}C excursion correlated to the Basal Cambrian Excursion (BACE) (Corsetti and Hagadorn, 2000).

In addition to the trace fossil *T. pedum*, *Rusophycus* was also found between the second and third dolomite marker beds of the lower member (Jensen et al., 2002). *Palaeophycus* and *Planolites* were reported from the first parasequence, below the lowermost dolomite marker bed, and *Helminthoidichnites* was reported from the second parasequence (Waggoner and Hagadorn, 2002). Other biostratigraphically significant ichnofossils including *Monomorphichnus*, *Rusophycus*, *Palaeophycus*, *Didymaulichnus miettensis*, and "*Taphrhelminthopsis" circularis* were reported from the uppermost parasequence—above the top dolomite marker bed—of the lower member Wood Canyon Formation (Corsetti and Hagadorn, 2000; Jensen et al., 2002). Reported bilobed arthropod trace fossils demarcate the *Rusophycus avalonesis* ichnofossil zone within the upper portion of the lower member of the Wood Canyon Formation. The reports of Ediacaran body fossils and euarthropod trace fossils within ~200 m of each other highlights the condensed nature of the lower member Wood Canyon Formation (Jensen et al., 2002).

Ediacaran–Cambrian Boundary Strata in the White-Inyo Ranges and Esmeralda County

In the White-Inyo Ranges and Esmeralda County, strata recording the terminal Ediacaran and Ediacaran–Cambrian boundary occur in the upper Reed Dolomite and Deep Spring Formation (Figs. 3B and 3C). In the White Mountains, the contact between the Reed Dolomite and the Deep Spring Formation is a sharp transition from recrystallized, massive dolostone to distinctly bedded dolostone, limestone, and fine-grained siliciclastic strata of the Deep Spring Formation (Albers and Stewart, 1972). These units were first defined in the White Mountains (named by Knopf, 1918), and thus the contact is easily identifiable here. In the Last Chance Range (Fig. 1) and Esmeralda County, however, this contact is more difficult to identify due to interbedded, fine-grained siliciclastic strata in the upper Reed Dolomite and variable dolomitization across this transition. Smith et al. (2016b) suggested that the base of the Deep Spring Formation should be marked by a regional exposure surface that is well exposed at Mt. Dunfee in Esmeralda County and that the interbedded limestone and dolostone beds beneath this surface be referred to as the "Reed-Deep Spring Transitional Beds." However, in most sections studied, the exposure surface is not easy

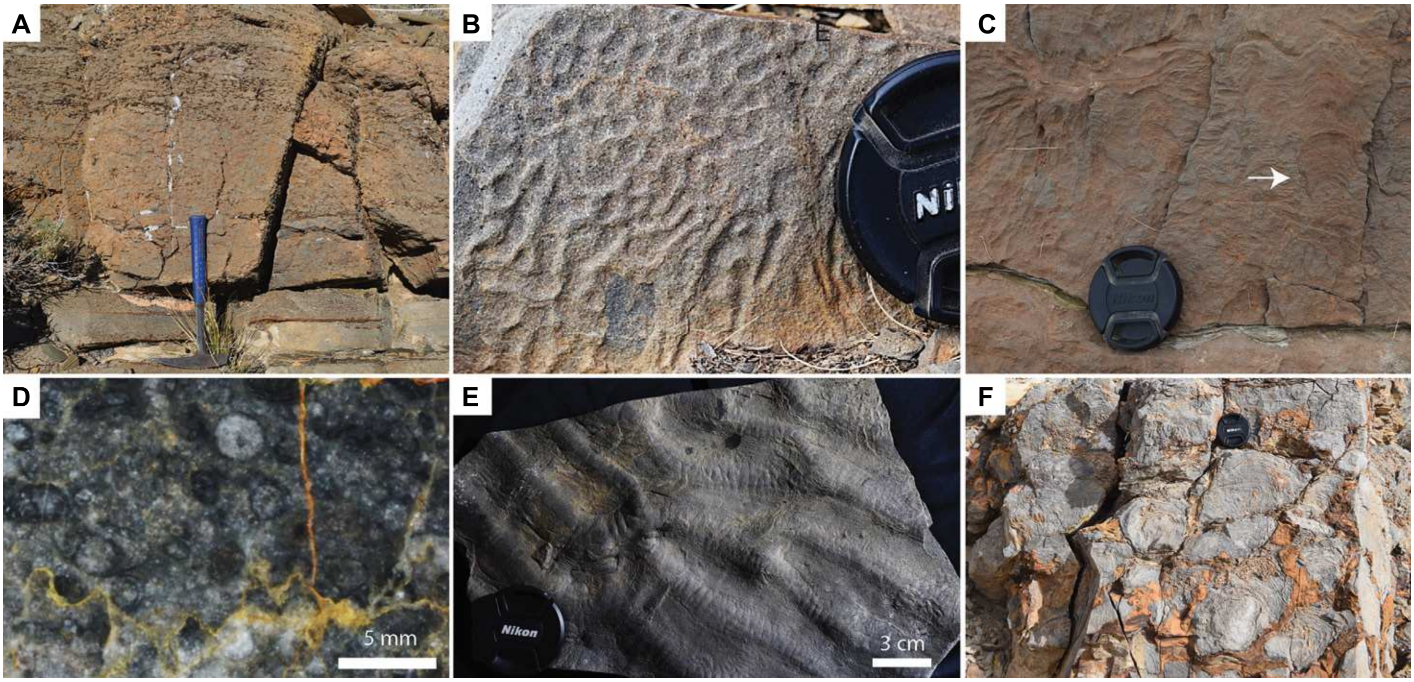

Figure 4. Photographs of microbial textures, microbialites, and ooids in Ediacaran–Cambrian boundary units in the southwest Great Basin are shown. (A) Thrombolite in the Dunfee Member of the Deep Spring Formation at Mt. Dunfee, Nevada. (B) An example of a microbially induced sedimentary structure; these are common in the fine-grained siliciclastics of the Deep Spring and lower Wood Canyon formations. (C) Stromatolites in the lowest marker bed of the lower Wood Canyon Formation in section north of Echo Canyon. White arrow marks stromatolite. (D) A polished slab with pisoids and ooids from a dolomite marker bed in the lower member of the Wood Canyon Formation in Titanothere Canyon. (E) A bedding surface with corrugated structures from the Inyo Mountains that are interpreted as microbial mat-bound ripples (reproduced from Nelson and Smith, 2019). (F) A stromatolitic reef horizon in the Esmeralda Member of the Deep Spring Formation at Mt. Dunfee, Nevada. These reefs are regionally consistent within the Esmeralda Member of the Deep Spring Formation, although with different morphologies and thicknesses among sections.

to identify, and the middle of the upper Reed Dolomite has distinct, heterolithic bedded facies that are likely correlative to the Hines Tongue in the White-Inyo Ranges. In structurally complex areas, interbedded limestone, dolostone, and fine-grained siliciclastic strata of the Reed Dolomite can easily be mistaken for the Dunfee Member of the Deep Spring Formation. Finally, not only are thick limestone beds present within the Reed Dolomite in some sections (i.e., Mt. Dunfee and Jupiter Mountain), but there is also increased dolomitization within the Deep Spring Formation in the more distal sections (i.e., Clayton Ridge), which further complicates confident lithostratigraphic identification of these units.

The top of the Reed Dolomite is a regional maximum regressive surface marked by localized paleokarst, and the base of the overlying Deep Spring Formation is claystone, mudstone, siltstone, and micaceous sandstone containing mud cracks, muds chips, trace fossils, and body fossils and deposited within a transgressive sequence. The Dunfee (lower) Member of the Deep Spring Formation is a 100–200-m-thick heterolithic unit that is composed primarily of gray to pale orange dolomitic limestone and limestone with minor dolostone, green to gray siltstone, calcareous sandstone, and quartzite (Albers and Stewart, 1972). The middle to upper part of the unit is predominantly cross-stratified limestone and clotted limestone beds that are interpreted as microbialites (Fig. 4E). Slump folds and load structures occur at stratigraphic horizons throughout the member. Pink to blue recrystallized dolostone of the uppermost Dunfee Member is sharply overlain by tan to green shoreface sandstone with mud cracks and abundant trace fossils of the basal Esmeralda Member. The contact is interpreted as a maximum regressive surface overlain by a transgressive sequence.

The Esmeralda (middle) Member of the Deep Spring Formation (Corsetti and Kaufman, 1994; Rowland and Corsetti, 2002; Ahn et al., 2012) is composed of quartzite and calcareous sandstone, stromatolitic and oolitic limestone, and minor siltstone and shale (Albers and Stewart, 1972). There are several intervals of microbial carbonates with morphologies that include inclined columnar stromatolites, broad hemispheroidal stromatolites, and thrombolites (Oliver, 1990; Oliver and Rowland, 2002). Oolite is abundant in the Esmeralda Member and, in some places, erosively cuts into underlying stromatolite beds (Oliver, 1990). Interbedded with some of the stromatolite and oolite beds are siliciclastic intervals of shale, siltstone, and sandstone, some of which preserve peritidal, wavy-bedded facies and storm deposits (Nelson and Smith, 2019). Siliciclastic intervals in the middle part of the Esmeralda Member of the Deep Spring Formation contain sedimentary features that are interpreted as microbially induced structures, including kinneyia-type wrinkle structures (Hagadorn and Bottjer, 1997, 1999) and other more enigmatic corrugated structures that are interpreted as microbial mat-stabilized heterolithic bedding (Nelson and Smith, 2019).

The Gold Point Member of the Deep Spring Formation sharply overlies the Dunfee Member and consists of gray-green siltstone to very fine quartz sandstone in the basal to middle part of the member. The upper part of the member is capped by a unit of recrystallized, light gray limestone to dolostone, which in turn is sharply overlain by brown to gray siltstone and sandstone of the Andrews Mountain Member of the Campito Formation. Both the tops of the Esmeralda and Gold Point members are interpreted to record subaerial exposures that are overlain by transgressive sequences.

The late Ediacaran fossil, *Cloudina*, occurs within the upper Reed Dolomite and the Dunfee Member of the Deep Spring Formation (Taylor, 1966; Mount et al., 1983; Gevirtzman and Mount, 1986; Signor et al., 1987; Grant, 1990). Ediacaran body fossils including *Gaojiashania*, *Conotubus*, *Wutubus*, and other unclassified, smooth-walled tubular fossils occur in two stratigraphic intervals in the Deep Spring Formation—in siliciclastic rocks of the basal Dunfee Member and the lower Esmeralda Member (Smith et al., 2016b). Similar to the cloudinomorphs from the Death Valley region, *Conotubus* fossils from Mt. Dunfee were reinterpreted as two separate cloudinid taxa: *Saarina* and *Costatubus* (Selly et al., 2020). Possible *Pteridinium* was reported from the Esmeralda Member of the Deep Spring Formation at the Molly Gibson Mine section in the White Mountains (Cloud and Nelson, 1966; Nelson and Durham, 1966). However, we could not confirm this report, and corrugated structures from this section and other correlative sections in the White-Inyo Ranges resembling erniettomorphs were instead interpreted as microbially mediated sedimentary structures (Nelson and Smith, 2019).

Simple, bed-planar trace fossils including *Helminthoidichnites* and *Planolites* occur in the Wyman Formation and the Hines Tongue of the Reed Dolomite (Stewart, 1970; Corsetti and Hagadorn, 2003). *Torrowangea* has also been reported from the Hines Tongue of the Reed Dolomite (Corsetti and Hagadorn, 2003). Relatively simple trace fossils, including *Helminthopsis*, *Helminthoidichnites*, *Planolites*, *Cochlichnus*, *Bergaueria*, and small treptichnids, are preserved within the siliciclastic rocks of the basal Dunfee Member of the Deep Spring Formation (Gevirtzman and Mount, 1986; Tarhan et al., 2020). The Esmeralda Member contains multiple horizons of simple surface trace fossils, and *T. pedum* occurs in the upper part of this unit (Gevirtzman and Mount, 1986; Corsetti and Hagadorn, 2000; Tarhan et al., 2020). The lowest report of *T. pedum*, and thus the local placement of the Ediacaran–Cambrian boundary, occurs above the nadir of a large negative $\delta^{13}C$ excursion that has been correlated with the BACE within the middle to upper part of the Esmeralda Member (Corsetti and Kaufman, 1994; Oliver and Rowland, 2002). The overlying Gold Point Member of the Deep Spring Formation contains the stratigraphically lowest arthropod trace fossils, including specimens classified as *Rusophycus, Cruziana,* and *Diplichnites* (Cloud and Nelson, 1966; Alpert, 1976). In Esmeralda County, the lowest stratigraphic occurrence of trilobites is in the lowermost Gold Coin Member of the Campito Formation, within a few meters of the boundary with the underlying Andrews Mountain Member (Hollingsworth, 2011). Trilobites, brachiopods, and hyoliths occur at several stratigraphic horizons in the Gold Coin and Montenegro members (Nelson, 1978; Signor and McMenamin, 1988; Hollingsworth, 2011).

Ediacaran–Cambrian Correlations in the Southwest Great Basin

Precise regional correlations between the more paleo-proximal Death Valley region and the paleo-distal White-Inyo Ranges and Esmeralda County have been hindered by the lack of radioisotopic ages, lack of exposure between the areas, and uncertainties in structural restorations. Nonetheless, Stewart (1970) proposed the first comprehensive lithostratigraphic correlation framework for the southern Great Basin as follows: the Deep Spring Formation is an offshore equivalent of the lower member of the Wood Canyon Formation; the Hines Tongue through the upper Reed Dolomite is equivalent to the upper siliciclastic Stirling Quartzite; and the lower Reed Dolomite is equivalent to the dolomitic "member D" of the Stirling Quartzite. The underlying Wyman Formation was tentatively correlated with the Johnnie Formation through the middle Stirling Quartzite. More recently, using chemostratigraphy and biostratigraphy, others have suggested instead that the Reed Dolomite and Dunfee Member of the Deep Spring Formation correlate with the Stirling Quartzite and that the Wyman-Reed unconformity correlates with the upper Johnnie Formation unconformity (Corsetti and Hagadorn, 2000). In this framework, the Hines Tongue of the Reed Dolomite correlates with the lower to middle Stirling Quartzite, and the Wyman Formation is correlative with the Johnnie Formation (Corsetti and Hagadorn, 2000).

Most of the lower member of the Wood Canyon Formation has been correlated to the Deep Spring Formation based on Ediacaran–Cambrian boundary lithostratigraphic, chemostratigraphic, and biostratigraphic correlations, with three dolostone marker beds of the lower member of the Wood Canyon Formation correlated to the carbonate-dominated units that cap each of the members of the Deep Spring Formation (Fig. 2; Stewart, 1970; Corsetti and Kaufman, 1994; Corsetti et al., 2000; Corsetti and Hagadorn, 2000; Jensen et al., 2002; Oliver and Rowland, 2002). The maximum regressive surface at the base of the middle member of the Wood Canyon Formation has been correlated with the base of the Campito Formation, which is consistent with the first occurrences of trilobites in the two regions (Stewart, 1970). This correlation is also consistent with detrital zircon age distributions and Nd isotope chemostratigraphy from these units (Gehrels et al., 1995; Farmer and Ball, 1997; MacLean et al., 2009; Chapman et al., 2015).

PALEONTOLOGICAL AND TAPHONOMIC RESULTS

Ediacaran body fossils were found in seven stratigraphic sections in five different taphonomic modes: calcification, two-dimensional pyritization (now iron oxides), three-dimensional pyritization, three-dimensional cast and mold preservation, and two-dimensional reflective compressional preservation (Fig. 5). In some cases, more than one taphonomic mode exists within a single fossiliferous interval. Below, we describe the different modes of preservation and their paleoenvironmental contexts.

Calcified Tubular Body Fossils

Calcified tubular body fossils in carbonate strata have been recognized in sections in the White-Inyo Ranges of California and Esmeralda County, Nevada, and were variably identified as *Wyattia*, *Nevadatubulus*, *Sinotubulites, Coleoloides,* and *Salanytheca* (Taylor, 1966; Cloud and Nelson, 1966; Mount et al., 1983; Signor et al., 1983; Signor et al., 1987) and then later reinterpreted as the late Ediacaran index fossil *Cloudina* (Grant, 1990; Yang et al., 2022). These fossils are recrystallized, which obscures much of the morphological detail and makes refined taxonomic assessment difficult. However, these are likely all members of the recently defined tubiform morphoclade of cloudinomorphs and perhaps similar to other better preserved pyritized tubular specimens from these units (Selly et al., 2020). Here, we do not attempt further taxonomic refinement to avoid future confusion in the literature and simply refer to them as calcified tubular fossils. The only locality in the Death Valley region in which calcified *Cloudina* fossils have been reported is in the member D of the Stirling Quartzite in the northern Funeral Range (Langille, 1974); in this study, we were unable to confirm this report, and no occurrences of Ediacaran calcified fossils were identified in the Death Valley region.

In the White-Inyo Ranges and Esmeralda County, calcified tubular fossils are reported from the upper part of the Reed Dolomite and from the Dunfee Member of the Deep Spring

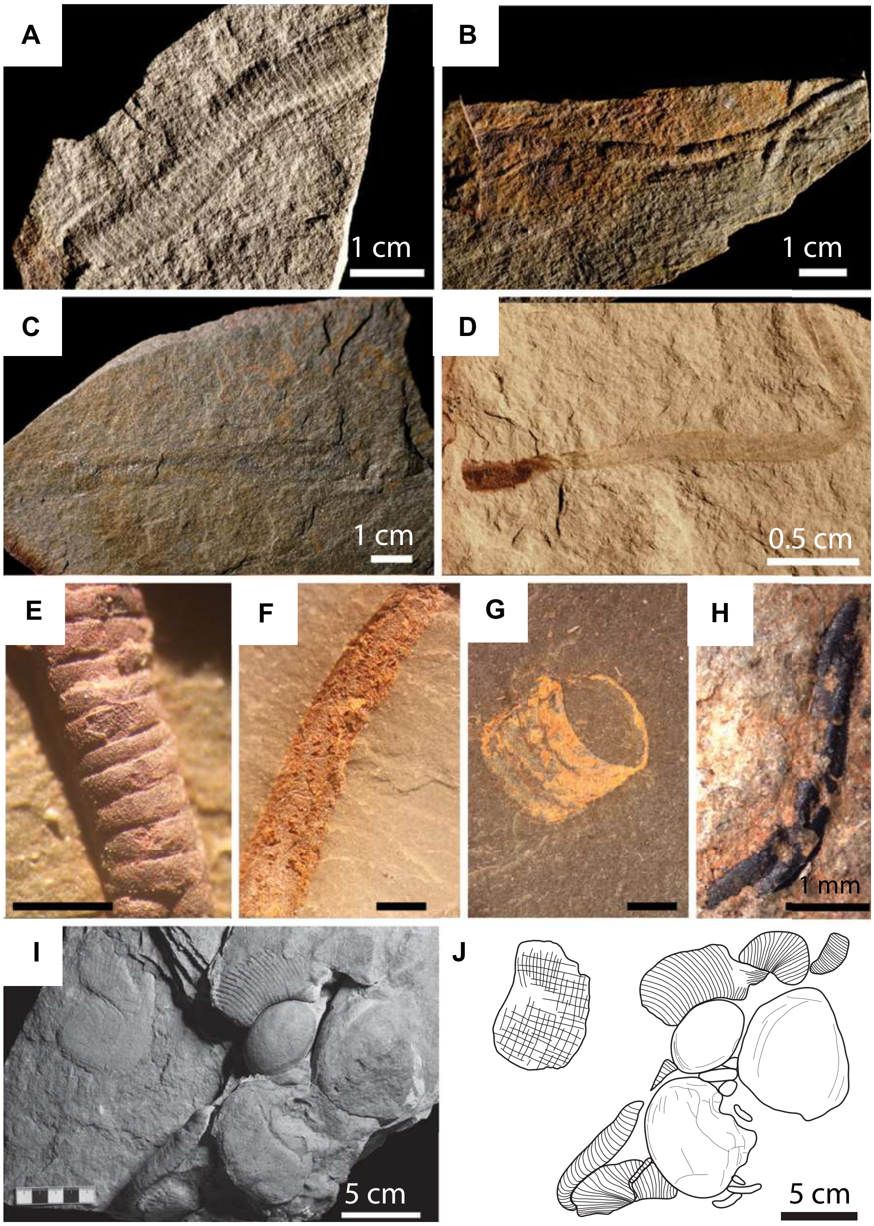

Figure 5. Examples are shown of Ediacaran body fossils and modes of preservation from the Death Valley Region and Esmeralda County. (A–B) Cast of mold preservation of annulated tubular fossils (identified as *Gaojiashania* [panel A] and *Wutubus* [panel B]) in siltstone and sandstone of the basal Dunfee Member of the Deep Spring Formation at Mt. Dunfee (reproduced from Smith et al., 2016b). (C) A tubular fossil preserved as a 2-D compression in siltstone. This specimen is from the same stratigraphic interval as in Figures 5A, 5B, and 5D in the basal Dunfee Member of the Deep Spring Formation at Mt. Dunfee. (D) Smooth-walled, tubular fossil preserved as a pyritized, 2-D compression. This specimen is from the same stratigraphic interval as in Figures 5A–5C (reproduced from Smith et al., 2016b). (E–G) Pyritized cloudinomorphs from the Esmeralda Member of the Deep Spring Formation at Dunfee show both 2-D and 3-D preservation from the same stratigraphic interval (E is reproduced from Smith et al., 2016b). (H) Pyritized *Corumbella* preserved in 3-D from the lower member of the Wood Canyon Formation at Montgomery Mountains (reproduced from Smith et al., 2017). Preservation both as 2-D compressions and 3-D preserved iron oxides was found at this locality. (I–J) Photograph and corresponding sketch of erniettomorphs and an unclassified cross-hatched fossil from the lower member of the Wood Canyon Formation at Montgomery Mountains (reproduced from Smith et al., 2017).

Formation in five localities (Figs. 6–7). No calcified tubular fossils have been identified in the stromatolite reefs of the Esmeralda Member of the Deep Spring Formation or anywhere stratigraphically higher than the uppermost beds of the Dunfee Member, which is consistent with the results of other workers who have studied these units (e.g., Gevirtzman and Mount, 1986; Smith et al., 2016b).

Regionally, calcified tubular fossil occurrences are not obviously widespread. They occur predominantly in carbonate grainstone and often as dark gray limestone lenses of shell debris wackestone to packstone (Fig. 6A). There are rare occurrences of scattered fossil debris within what are interpreted as small, recrystallized thrombolite reefs (Fig. 4A) in the Dunfee Member. Additionally, rare, calcified tubular fossils are found within red-brown, originally glauconitic, peloidal packstone of the Dunfee Member and uppermost Reed Dolomite (Stewart, 1970; Gevirtzman and Mount, 1986). The best preservation of calcified tubular fossils in the region occurs near Mt. Dunfee and the area to the east of Mt. Dunfee, although even there, the fossils are coarsely recrystallized. In a few places around Mt. Dunfee, there are isolated examples of <4-cm-thick shell beds in which individual tubes are <4 cm in length (Fig. 6B); within these beds the fossils are dominantly intact, which suggests that these shells were not subject to significant transport.

Cast and Mold Preservation

Fossils preserved through cast and mold preservation are separated into two sub-categories: moldic preservation of erniettomorphs in micaceous sandstone (e.g., Smith et al., 2017; Runnegar, 2021) and casts and molds of tubular fossils in claystone, mudstone, siltstone, and micaceous sandstone (e.g., Hagadorn and Waggoner, 2000; Smith et al., 2016b, 2017). This distinction is made because the interpreted preservational mechanisms differ. The three-dimensional preservation of erniettomorph fossils is due to sediment infilling the organism prior to burial (e.g., Seilacher, 1992), while the three-dimensional casts and molds of the tubular fossils are due to early mineral precipitants templating to labile tissue (e.g., Petrovich, 2001; Newman et al., 2019). Three-dimensional moldic preservation or endorelief preservation of soft-bodied erniettomorphs is present in the lower part of the lower member of the Wood Canyon Formation, but these fossils are extremely rare in southwestern Laurentia, and there are only a few examples of well-preserved, undisputed erniettomorphs (Smith et al., 2017; Runnegar, 2021).

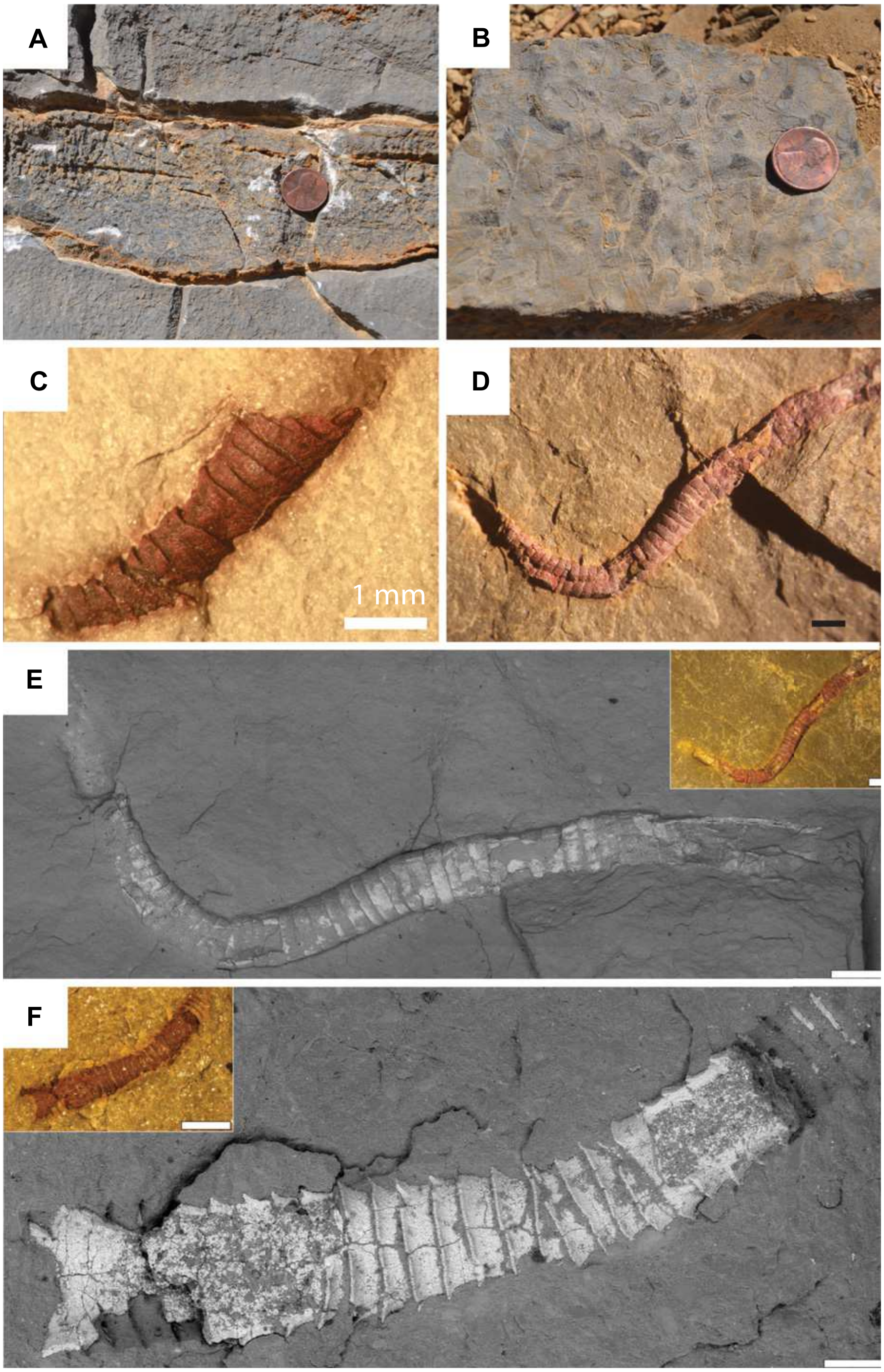

Figure 6. Cloudinomorphs from latest Ediacaran strata in California and Nevada are shown. (A) Lag deposit of cloudinomorph shell hash (middle of photograph) from the upper Reed Dolomite at Mt. Dunfee. White spots are hammer marks on the outcrop. (B) Bedding surface of *Cloudina* fossils from the upper Reed Dolomite at Mt. Dunfee. (C) Pyritized cloudinomorph *Saarina hagadorni* from the lower member of the Wood Canyon Formation at Montgomery Hills (reproduced from Smith et al., 2017). (D) Cloudinomorph from the Esmeralda Member of the Deep Spring Formation at Mt. Dunfee. Specimen was first identified as *Conotubus* (Smith et al., 2016b) but later reinterpreted as *Costatubus bibendi* (Selly et al., 2020). (E) Scanning electron microscopy (SEM) with light microscopy insets of *Costatubus bibendi* holotype (reproduced from Selly et al., 2020). (F) SEM image with light microscopy inset of *Saarina hagadorni*, another cloudinomorph, from the same stratigraphic horizon as the specimen in Figures 6D–6E (reproduced from Selly et al., 2020).

In both the Death Valley region and Esmeralda County, casts and molds of tubular body fossils are found in fine-grained siliciclastic strata above maximum regressive surfaces within the basal transgressive sequence. These intervals demonstrate sedimentological evidence for high rates of sediment accumulation, including load casts, convolute laminations, and mud chip rip ups. At Mt. Dunfee and in the Montgomery Mountains, some casts and molds of tubular fossils are found on the same bedding surfaces as mud chip rip ups and thus were interpreted as transported (Smith et al., 2016b, 2017). These fossiliferous horizons are interpreted as deposited within shallow marine, peritidal environments. Cast and mold preservation of tubular fossils is found in the same stratigraphic intervals containing two other taphonomic modes: reflective two-dimensional compression and pyritization.

Reflective Two-Dimensional Compressions of Tubular Body Fossils

Reflective, micaceous two-dimensional compressions of tubular fossils are found on siltstone and micaceous fine-grained sandstone at Mt. Dunfee and in the Montgomery Mountains in the basal Dunfee Member and the basal Wood Canyon Formation, respectively (Hagadorn and Waggoner, 2000; Smith et al., 2016b, 2017). They are preserved on bedding surfaces of siltstone to fine-grained, micaceous sandstone. Like some of the fossils preserved as casts and molds, fossils preserved in this taphonomic mode are found on and interbedded with beds containing redeposited mud chip rip-ups. Unlike the three-dimensional cast and mold preservation of tubular body fossils found in the same stratigraphic intervals, fossils preserved in this mode are only found within siltstone and fine-grained sandstone and never in mudstone. While these tubular specimens lack annulations or any internal structures, they fall within the same width and length ranges as the three-dimensional casts and molds, which suggests they are similar taxa preserved in a different taphonomic mode. The two-dimensional preservation is far less common than the three-dimensional cast and mold preservation, perhaps in part because these specimens are more difficult to find in the field.

Tubular Fossils Preserved as Iron Oxides

Organisms preserved as two- and three-dimensional, pyritized (now iron oxide) tubes are found in five stratigraphic sections across the basin (Figs. 6–7; Smith et al., 2016b, 2017). Although no original pyrite has been reported from these specimens, the fossils are interpreted as being preserved through light to pervasive

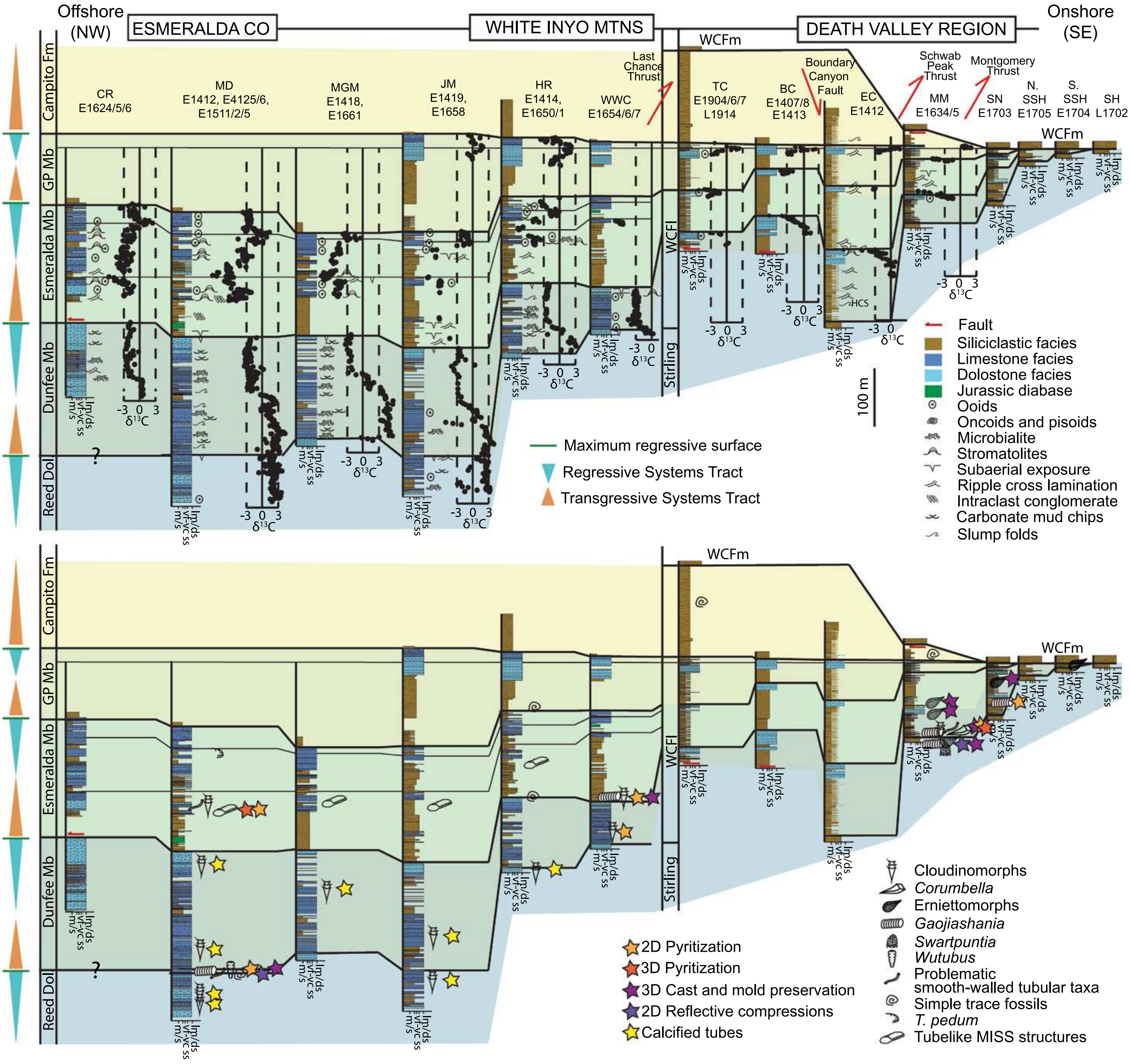

Figure 7. Measured sections of late Ediacaran through Cambrian strata from the proximal Death Valley region to the more distal Esmeralda County. In the upper panel, carbonate carbon isotope chemostratigraphic data are plotted next to measured stratigraphic sections. Colored polygons show interpreted correlations between sections. Datum is the 0‰ $\delta^{13}C$ crossing point above the Basal Cambrian Excursion within the upper carbonate units of the lower member (Mb) Wood Canyon Formation (Fm) and the Deep Spring Formation. In the lower panel, Ediacaran fossil occurrences and their modes of preservation are shown. Carbon isotope data from the Mt. Dunfee and Echo Canyon sections were previously published in Smith et al. (2016b) and Smith et al. (2017), respectively. GP—Gold Point Member. Abbreviations for measured sections: BC—Boundary Canyon; CR—Clayton Ridge; EC—north of Echo Canyon; HR—Hines Ridge; JM—Juniper Mountain; MD—Mt. Dunfee; MGM—Molly Gibson Mine; SH—Silurian Hills; SN—Southern Nopahs; MM—Montgomery Mountains; SSH—Salt Spring Hills; TC—Titanothere Canyon; WWC—Whippoorwill Canyon.

pyritization of tubular fossils that were subsequently oxidized by diagenetic fluids (Smith et al., 2016b, 2017; Selly et al., 2020; Schiffbauer et al., 2020), similar to the preservation of tubular fossils in the Gaojiashan Laggerstätte (Cai and Hua, 2007; Cai et al., 2012). The most abundant and well-preserved examples of two- and three-dimensional, pyritized tubular fossils are concentrated in two stratigraphic intervals: (1) fine-grained siliciclastic strata in the lower member of the Wood Canyon Formation, below the lowest dolostone marker bed, and

(2) fine-grained siliciclastic beds in the middle Esmeralda Member of the Deep Spring Formation (Fig. 7; Smith et al., 2016b, 2017).

In the Montgomery Mountains in the Death Valley region, hundreds of iron oxide-replaced fossils were found in the lower member of the Wood Canyon Formation, below the lowest carbonate marker bed, in green, powdery claystone and mudstone, green to tan siltstone, and micaceous, very fine- to medium-grained sandstone (Smith et al., 2017). Additional occurrences of iron oxide-replaced tubular fossils within this stratigraphic interval were found in the Spring Mountains and the southern Nopah Range (Fig. 7). At Mt. Dunfee, a few two-dimensional, lightly pyritized, smooth-walled tubular fossils were found in the Dunfee Member of the Deep Spring Formation (Smith et al., 2016b). These fossils were found in the same stratigraphic interval as the casts and molds and reflective compressions of Ediacaran tubular body fossils that include *Gaojiashania* and *Wutubus* (Smith et al., 2016b)—within a transgressive sequence above the exposure surface at the top of the Reed Dolomite.

A second stratigraphic interval in the Esmeralda Member of the Deep Spring Formation contains hundreds of two- and three-dimensional, pyritized fossils that were originally called *Conotubus* (Smith et al., 2016b) and later taxonomically classified as *Saarina* and *Costatubus* (Selly et al., 2020). These fossils are found on at least five bedding planes of black to tan mudstone and siltstone within a 3 m stratigraphic interval. *Elainabella*, a purported Ediacaran algal fossil (Rodriguez and Rowland, 2014), was found in the same stratigraphic interval at this site. Additional rare occurrences of pyritized Ediacaran tubular fossils within this stratigraphic interval were found in Whippoorwill Wash in the Inyo Range (Fig. 7). Across the region, this stratigraphic interval preserved microbially induced sedimentary structures (Nelson and Smith, 2019).

CHEMOSTRATIGRAPHIC RESULTS

Carbon and oxygen isotopes of carbonates ($\delta^{13}C$ and $\delta^{18}O$) were measured in 10 composite Ediacaran–Cambrian sections across the Great Basin (Fig. 7). In all sections, there is a broad, negative carbon isotope excursion that is superimposed with smaller scale variability. These results demonstrate trends similar to those of previously published $\delta^{13}C$ data from this region (Corsetti and Hagadorn, 2000, 2003; Smith et al., 2016b, 2017) and demonstrate lateral stratigraphic reproducibility in Ediacaran–Cambrian carbon isotope values across the southern Great Basin.

In the Death Valley region, carbonate $\delta^{13}C$ and $\delta^{18}O$ data were produced from four measured sections of the lower member of the Wood Canyon Formation (Montgomery Mountains, north of Echo Canyon, Boundary Canyon, and Titanothere Canyon). In the lowermost dolostone marker bed, there is a general downward trend in $\delta^{13}C$ from values that start around $\sim+1‰$ to values that reach $\sim-6‰$, with smaller negative excursions superimposed to produce a sawtooth pattern (Fig. 7). The middle dolostone marker bed has $\delta^{13}C$ values that are all ^{13}C-depleted, with values ranging from $\sim-1‰$ to $-4.5‰$. The top dolostone marker bed has $\delta^{13}C$ values that are as low as $\sim-3‰$ at its base, which rise to $\sim+2‰$ before dropping to $\sim0‰$ (Fig. 7). The minimum and maximum $\delta^{18}O$ values are $-14.3‰$ and $-5.5‰$, respectively. There is no strong covariation between $\delta^{18}O$ and $\delta^{13}C$ values (R^2 for all samples $= 0.015$; Fig. S1; see footnote 1), and a cross plot of $\delta^{13}C$ and $\delta^{18}O$ values is shown in Fig. S1.

In the White-Inyo Ranges and Esmeralda County, six composite measured sections have accompanying carbonate $\delta^{13}C$ and $\delta^{18}O$ data (Fig. 7). The composite section from Mt. Dunfee was previously published by Smith et al. (2016b) and is the section that was sampled at the highest resolution. Like the sections in the Death Valley region, chemostratigraphic data across this region are reproducible (Fig. 7). In all sections, strata of the upper Reed Dolomite record $\delta^{13}C$ values between $\sim0‰$ and $+4‰$. In the Dunfee Member of the Deep Spring Formation, $\delta^{13}C$ values decrease from $\sim+3‰$ to $+5‰$ to $\sim-3‰$ and remain consistent throughout the upper part of the Dunfee Member. The lowest limestone beds of the Esmeralda Member have $\delta^{13}C$ values of $\sim-6‰$ to $-3‰$. Above this, the $\delta^{13}C$ values decrease to a nadir of $\sim-8‰$ to $-6‰$. Above the nadir, the $\delta^{13}C$ values increase to $+1‰$. In the upper Esmeralda Member, the $\delta^{13}C$ values are $\sim-3‰$ to $-2‰$. The carbonates of the Gold Point Member have $\delta^{13}C$ values that are $-2 - 0‰$ at the base, trend positive to values $<+3‰$, then decrease again to reach values of $\sim-3‰$. Despite changes in sedimentary facies, variations in carbonate content, and differences in metamorphic grade among sections, the $\delta^{13}C$ values are reproducible across the White-Inyo Ranges and Esmeralda County (Fig. 7). In this region, co-variation of $\delta^{13}C$ and $\delta^{18}O$ values is marginally higher than in the Death Valley region ($R^2 = 0.140$) but not significant enough to indicate that the $\delta^{13}C$ values were altered by meteoric diagenesis. Crossplots for $\delta^{13}C$ and $\delta^{18}O$ values from this region are shown in Fig. S2 (see footnote 1).

DISCUSSION

Ediacaran Body Fossil Taphonomy in the Southwestern USA

The different taphonomic windows of Ediacaran body fossil preservation and the lateral extent of preservation of latest Ediacaran strata across the southwestern U.S. allow for placement of Ediacaran fossils into a paleogeographic and sequence stratigraphic context that spans thousands of square kilometers of a fluvial-deltaic to shallow marine latest Ediacaran continental margin (Fig. 7). Such a framework can be used to better understand the environmental setting of these late Ediacaran ecological communities as well as the processes and depositional settings that contributed to fossil preservation.

Calcified Tubular Fossils

Calcified tubular fossils are found in five localities in this study, but none of these demonstrate evidence that cloudinomorphs were metazoan reef builders (*contra* Penny et al., 2014). The calcified fossil occurrences in this region instead support the model that Ediacaran cloudinomorph aggregates are detrital buildups (e.g., Mehra and Maloof, 2018). The occurrences of pyritized cloudinomorphs within the more paleo-proximal siliciclastic beds of the lower Wood Canyon Formation and in lenses within the more distal carbonate platforms suggest that these organisms were living in a variety of shallow marine environments with multiple taphonomic pathways to preservation.

Ernietta Moldic Preservation

Three-dimensional moldic preservation or endorelief preservation of soft-bodied erniettomorphs is present in the lower part of the lower member of the Wood Canyon Formation, but these fossils are extremely rare in southwestern Laurentia, and there are only a few examples of well-preserved, undisputed erniettomorphs from one locality (Smith et al., 2017; Runnegar, 2021). The composition of clay and quartz-rich sediment infill was suggested to play a critical role in enabling exceptional preservation (Hall et al., 2020). In this proposed taphonomic pathway, clay minerals adsorbed to organic surfaces during microbially mediated decay and helped to preserve carbonaceous material at the interface of the organism and the surrounding matrix. The quartz-rich infill of the fossils may have prevented flattening of the organism, and in turn, helped to retain the three-dimensional structure of its millimeter-scale features (Hall et al., 2020)—comparable to previous models for erniettomorph preservation (e.g., Dzik, 1999). Preservation requires not only rapid burial and minimal transport, but also infilling of the organism with texturally mature and compositionally immature siliciclastic sediment. This model helps to explain the global restriction of erniettomorph fossils to shallow marine to deltaic paleoenvironments and specific sedimentary facies (Germs, 1983; Grazhdankin, 2004; Bouougri et al., 2011; Maloney et al., 2020), as well as the general scarcity of these fossils in late Ediacaran strata. Detailed paleontological studies and computational fluid dynamics modeling have shown that *Ernietta* lived at least partially infaunally, with a small portion of the organism extended above the sediment-water interface (Ivantsov et al., 2016; Gibson et al., 2019, 2021); this life mode has been suggested as another important factor in preservation.

Cast and Molds and Two-Dimensional Reflective Tubular Body Fossils

Cast and mold preservation has been described from many Ediacaran-aged assemblages globally (e.g., Tarhan et al., 2016; MacGabhann et al., 2019, and references therein), and a number of models have been proposed to explain different pathways for preserving three-dimensional casts and molds of soft tissue. The "death mask" model (Gehling, 1999; Liu, 2016) suggests that sulfate-reducing bacteria facilitated the precipitation of a pyrite crust on the surface of decaying Ediacaran organisms. A separate mechanism invokes the role of early stage precipitation of silica cements enhanced by the high silica saturation state of Ediacaran oceans (Tarhan et al., 2016; Slagter et al., 2021). Alternatively, taphonomy experiments have demonstrated the importance of clay-microbe interactions in delaying decay and preserving soft-bodied organisms in clay-rich sediments (Darroch et al., 2012; Wilson and Butterfield, 2014; McMahon et al., 2016; Gibson et al., 2018; Naimark et al., 2018; Newman et al., 2019).

In the southwestern U.S., late Ediacaran cast and mold tubular fossils are found in clay-rich, fine-grained siliciclastic strata that are interpreted to have been deposited with high sediment accumulation rates in the intertidal zone and within the transgressive sequence that overlies regional exposure surfaces (Fig. 7). All specimens are preserved in endorelief, in which both part mold and counterpart cast are preserved, and some of these fossils are found in the same stratigraphic intervals as fossils preserved as two-dimensional, reflective tubular fossils and as pyritized fossils. Microbially induced sedimentary structures were not identified on bedding surfaces preserving fossils, but these structures are generally abundant within the fossiliferous intervals. Combined, these observations from the specimens in southwestern Laurentia are consistent with a taphonomic model in which the precipitation of early authigenic clays via clay-microbe interactions and rapid burial played important roles in the preservation of these soft-bodied Ediacaran organisms.

Pyritized Tubular Fossils

Pyritized fossils are thought to form through authigenic interactions during the degradation of organic matter from the decaying organism by sulfate-reducing bacteria within anoxic pore waters that have reduced iron as well as available sulfate (e.g., Schiffbauer et al., 2020). An unusual feature of the Wood Canyon pyritized tubular fossils is that, in some cases, the pyritization process ceased prior to complete pyritization—perhaps due to limitation of sulfate or reduced iron—resulting in preservation of internal soft tissue (Schiffbauer et al., 2020). The narrow balance between sulfate and ferrous iron concentrations necessary to form these fossils may have been sustained within a depositional setting that oscillated between anoxic and oxic bottom and/or pore waters.

All of the pyritized Ediacaran fossils from the southern Great Basin are found in mudstone, siltstone, and fine-grained micaceous sandstone that are interpreted to have been deposited in shallow paleoenvironments (<10 m of water depth), as evidenced by bedding surfaces above, below, and in correlative sections that contain mud cracks, interference ripples, and stromatolites (Fig. 7). The geochemical conditions necessary to preserve pyritized, tubular body fossils—particularly anoxic bottom and/or pore waters in very shallow environments—could have been achieved through partial restriction in lagoonal paleoenvironments.

To summarize, the taphonomies of late Ediacaran fossils within the regional context of this sedimentary basin highlight the increased preservational potential within specific paleoenvironments and stratigraphic sequences. Within shallow marine environments, there is enhanced preservational potential for soft-bodied organisms in the basal strata of transgressive sequences. Within these sequences, clay-rich sediments and high rates of sediment accumulation may have served as important background conditions for the facilitation of mineral-microbe interactions and/or pore fluid conditions critical to these taphonomic pathways.

Carbon Isotope Chemostratigraphy across the Ediacaran–Cambrian Boundary of Southwestern Laurentia

Carbon isotope data from 10 sections across the Ediacaran–Cambrian Great Basin demonstrate reproducibility of a large negative $\delta^{13}C$ excursion and of smaller scale chemostratigraphic perturbations, such as those documented in the middle and upper marker beds of the lower member of the Wood Canyon Formation (Fig. 7). The $\delta^{13}C$ chemostratigraphic profiles are reproducible despite changes in the carbonate content of sections, variable dolomitization, and sedimentary facies change (Fig. 7). In the lower Wood Canyon Formation, all carbonate beds are dolostone but vary in thickness and sedimentology among sections. Nonetheless, the carbon isotope shifts are consistent among the four Wood Canyon Formation sections with $\delta^{13}C$ data (Fig. 7).

Sections of the Deep Spring Formation vary in terms of facies, carbonate content, and carbonate mineralogy, particularly in the Dunfee and Esmeralda members. Although the top of the Dunfee Member is always dolomitized, in some sections (e.g., Clayton Ridge), almost the entire unit is dolomitized. The Esmeralda Member varies in both carbonate content and degree of dolomitization, and only the more distal sections contain dolostone beds. Additionally, the number of stromatolite beds increases and the number of limestone intraclast conglomerate beds decreases in the more outboard sections. Despite these differences in facies, all sections analyzed have broadly similar $\delta^{13}C$ profiles.

The negative $\delta^{13}C$ excursion recorded in the lower member of the Wood Canyon Formation and in the Dunfee and Esmeralda members of the Deep Spring Formation previously was correlated to the BACE and presumed to record a global negative carbon isotope excursion (Corsetti and Kaufman, 1994; Corsetti and Hagadorn, 2000; Smith et al., 2016b). However, studies on other shallow-water carbonate platforms have demonstrated that $\delta^{13}C$ values of carbonate strata can be records of changes in local mineralogy and/or early diagenesis rather than records of secular changes in the isotopic composition of global seawater (e.g., Swart and Eberli, 2005; Swart, 2008; Higgins et al., 2018). Even if certain carbon isotope excursions are regionally and globally reproducible, it has been demonstrated that these secular shifts in $\delta^{13}C$ values can be the result of sea-level–driven diagenesis (e.g., Ahm et al., 2019; Jones et al., 2020). In addition, other studies have shown that significant carbon isotopic shifts can correlate with dolomitization fronts (Bold et al., 2020; Nelson et al., 2021). Here, laterally variable dolomitization does not appear to have noticeably affected the $\delta^{13}C$ values of these strata. Cross plots of $\delta^{18}O$ versus $\delta^{13}C$ of these carbonates do not support a diagenetic origin for the observed secular changes related to meteoric fluids (Figs. S1–S2 ; see footnote 1). Furthermore, this $\delta^{13}C$ excursion spans a number of regionally significant sequence boundaries, which indicates that sea level may not have played a primary role in producing the carbon isotope shift. While the results from this study do not elucidate the cause(s) of the $\delta^{13}C$ excursions present in the Wood Canyon and Deep Spring formations, they demonstrate that its driver(s) must have been regionally extensive, if not global. Even if $\delta^{13}C$ values of these units are recording isotopic values of local and/or diagenetic fluids, future interpretations must account for the regional reproducibility of the signal across ~250 km in California and Nevada or ~700 km (with great uncertainty due to debated paleogeographic restorations) if correlative sections along strike in northern Mexico are also considered (Hodgin et al., 2021).

Regional Correlations and Tectonic Setting

The lithostratigraphy, biostratigraphy, and chemostratigraphy presented here further support previous correlations between the Death Valley and Inyo facies for the Ediacaran–Cambrian boundary units (Figs. 2, 7, and 8; e.g., Stewart, 1970). Correlations that rely only on chemostratigraphic data for the upper parts of the lower Wood Canyon Formation and Deep Spring Formation are equivocal; the upper dolostone marker bed of the lower Wood Canyon Formation could be correlated to the upper carbonate unit of the Esmeralda Member or the carbonate unit of the Gold Point Member. However, lithostratigraphy and previously published biostratigraphic data (Jensen et al., 2002) support a correlation of the three dolostone marker beds of the lower member of the Wood Canyon Formation to the carbonate-dominated upper units of each member of the Deep Spring Formation (Figs. 2, 7, and 8). Correlations among the older Ediacaran units remain uncertain. Although the Wyman Formation has been correlated with the Johnnie Formation (Corsetti and Hagadorn, 2000), the Shuram carbon isotope excursion has not been documented in the Wyman. One possible explanation for the lack of the Shuram excursion is that, during this time, deposition in this part of the basin was dominated by fine-grained, siliciclastic sediment. Another possibility is that the Wyman Formation correlates to the uppermost part of the Johnnie Formation, above the Shuram excursion.

Based on regional stratigraphic patterns, geologic mapping, sedimentology, and paleoflow indicators of Tonian and Cryogenian units in the Death Valley region, it has been suggested that deposition of these strata occurred within semi-restricted, tectonically active fault-bound basins (Miller, 1985; Smith et al., 2016a; Nelson et al., 2020). Overlying the laterally variable Tonian to early Ediacaran units are more continuous mid(?)–late Ediacaran–Cambrian units of the southern Great Basin that were deposited during more regionally consistent subsidence that is indicative of widespread rifting followed by lithospheric thermal contraction (Armin and

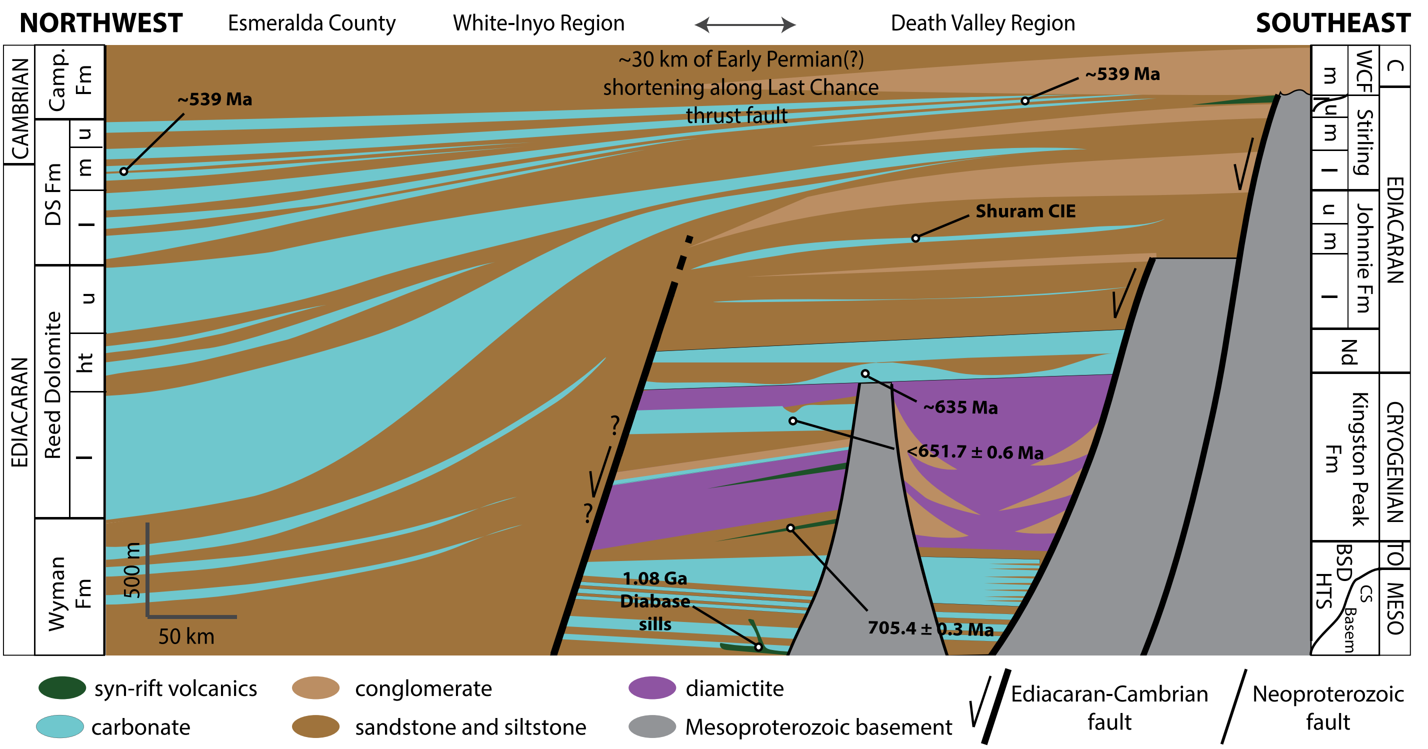

Figure 8. Schematic southeast to northwest transect of basin shows proposed correlations between the Death Valley region and the White-Inyo Ranges within a tectonic framework. The 1.08 Ga age on the Crystal Spring Formation (Fm) diabase is from Heaman and Grotzinger (1992). Cryogenian radioisotopic ages are from Nelson et al. (2020); the ca. 635 Ma age is based on correlation of the Noonday Formation to other Marinoan cap carbonate sequences (e.g., Prave et al., 1999), and the ca. 539 Ma age is based on correlation to the dated section in northern Mexico (Hodgin et al., 2021). Depiction of basement highs hinges upon models and reconstructions by Wright et al. (1976) and Stewart (1983). Note the syn-rift volcanics in the southeastern part of the basin; although no mantle-tapping plumbing system has been identified, regionally, the Ediacaran–Cambrian faults could have acted as conduits for volcanism. Note the vertical exaggeration. Meso—Mesoproterozoic; To—Tonian; C—Cambrian; Basem—basement; CS—Crystal Spring Formation; BSD—Beck Spring Dolomite; HTS—Horse Thief Spring Formation; Nd—Noonday Formation; WCF—Wood Canyon Formation; Camp—Campito Formation; DS Fm—Deep Spring Formation; l—lower; m—middle; u—upper; CIE—carbon isotope excursion.

Mayer, 1983; Levy and Christie-Blick, 1991). These regional subsidence patterns have been suggested to reflect a tectonic evolution from pulses of failed rifting during Tonian through early Ediacaran to the establishment of a rifted continental margin by the late Ediacaran (Bond et al., 1985; Prave, 1999; Nelson et al., 2020).

Consistent with these subsidence models, mid(?)–late Ediacaran to early Cambrian, rift-related faulting established the northwest-dipping continental margin with subsequent seafloor spreading leading to an early Cambrian rift-drift transition in southwestern Laurentia. Due to a dearth of Ediacaran radioisotopic ages in the region and the resulting difficulty in recognizing and temporally constraining disconformities and unconformities in these strata, the stratigraphic horizons marking the transition from an active to a passive margin have been long debated, although surfaces at the bases of and within the Johnnie Formation, Stirling Quartzite, and Wood Canyon Formation all have been proposed as possible candidates (Levy and Christie-Blick, 1991; Summa, 1993; Fedo and Cooper, 2001; Clapham and Corsetti, 2005). All of the exposed strata in the White-Inyo Ranges have been interpreted to record deposition on a rifted continental margin (e.g., Stewart, 1970).

A possible location for a major late Ediacaran to Cambrian rift shoulder is at the break between the Death Valley and White-Inyo facies belts, which follows the interpreted trace of the east-vergent Last Chance thrust fault (Figs. 1 and 8). It has been suggested that the Last Chance thrust is an example of décollement-style thrust faulting in a previously undeformed shale basin (Stevens and Stone, 2005). It is plausible that this shale basin of the Wyman Formation was deposited on the hanging wall of a major NW-dipping rift fault that formed the shelf edge of the incipient passive continental margin. Subsequently, the Permian Last Chance thrust fault(s) reactivated this late Ediacaran normal fault and transported the White-Inyo facies belt craton-ward toward the Death Valley facies belt (Fig. 8). In this model, the initiation of sedimentation in the White-Inyo Ranges and Esmeralda County would have coincided with active rift tectonism during Johnnie time (mid–late Ediacaran). Without subsurface data or an exposed base to the Wyman Formation, interpretation of the Last Chance thrust as a reactivated Ediacaran normal fault is speculative, but it explains the observed regional break in facies and provides a plausible location for a major late Ediacaran rift shoulder (Fig. 8).

Rift-Related Basalt Volcanism in Southwestern Laurentia

Ediacaran to Cambrian mafic volcanic rocks are documented in several sections in the southwestern U.S. (Fig. 9–10) (Morris et al., 1961; Kellogg, 1963; Stewart, 1970; Crittenden and Wallace, 1973; Stewart, 1974) and in Sonora, northern Mexico (Stewart et al., 1984; Barrón-Díaz et al., 2019a; Barrón-Díaz et al., 2019b; Hodgin et al., 2021). Ediacaran–Cambrian basalts in sections near Caborca in northern Mexico are some of the thickest (>60 m) exposed regionally (Stewart et al., 1984; Barrón-Díaz et al., 2019a). An epiclastic bed above some of the lowest basalt horizons that are exposed in the La Ciénega Formation yielded a maximum depositional age of 539.40 ± 0.23 Ma using U-Pb CA-ID-TIMS on zircon (Fig. 10; Hodgin et al., 2021). This provides a maximum age for the thicker intervals of basalt and volcaniclastics that occur within the overlying Cerro Rajón

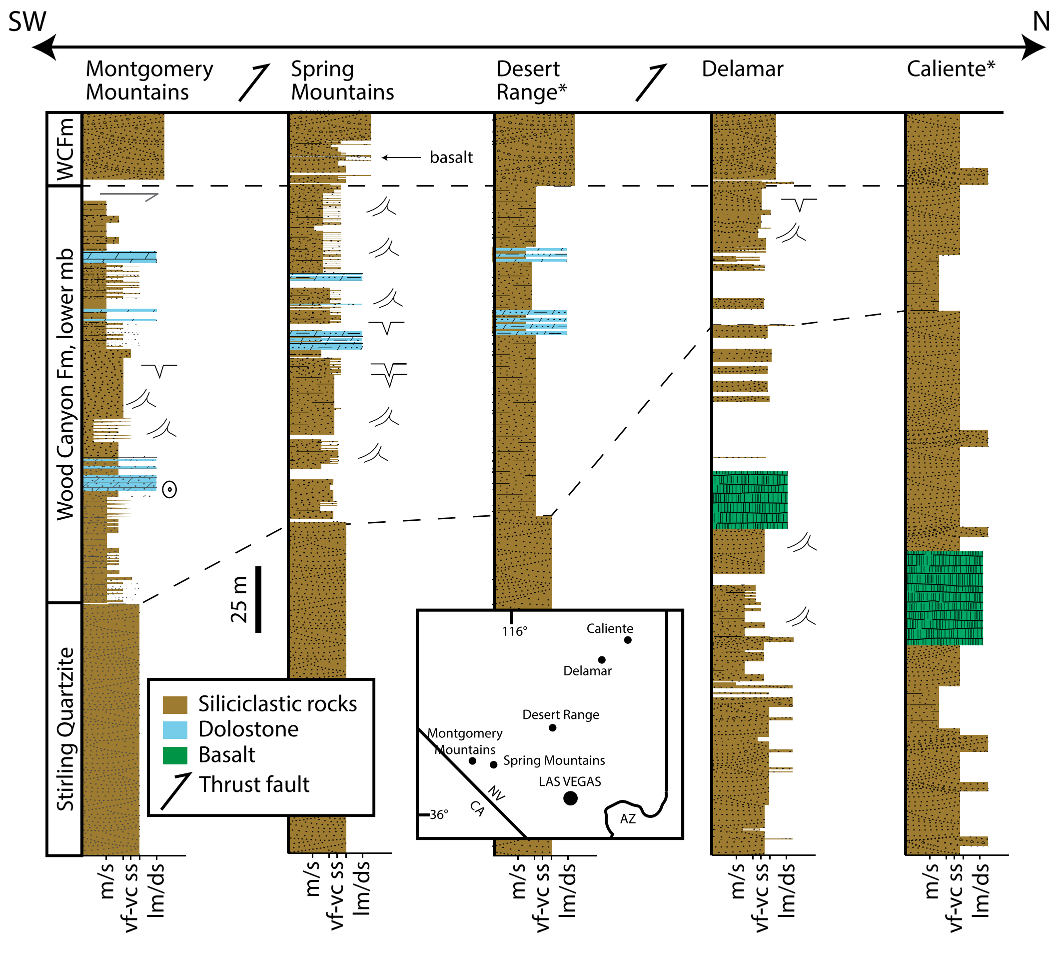

Figure 9. Northeast to southwest transect of Ediacaran–Cambrian sections in Nevada is shown. Three of these sections have basalt flows within Ediacaran–Cambrian strata. The two asterisked sections are replotted from Stewart (1974). Fm—formation; mb—member; AZ—Arizona; CA—California; NV—Nevada.

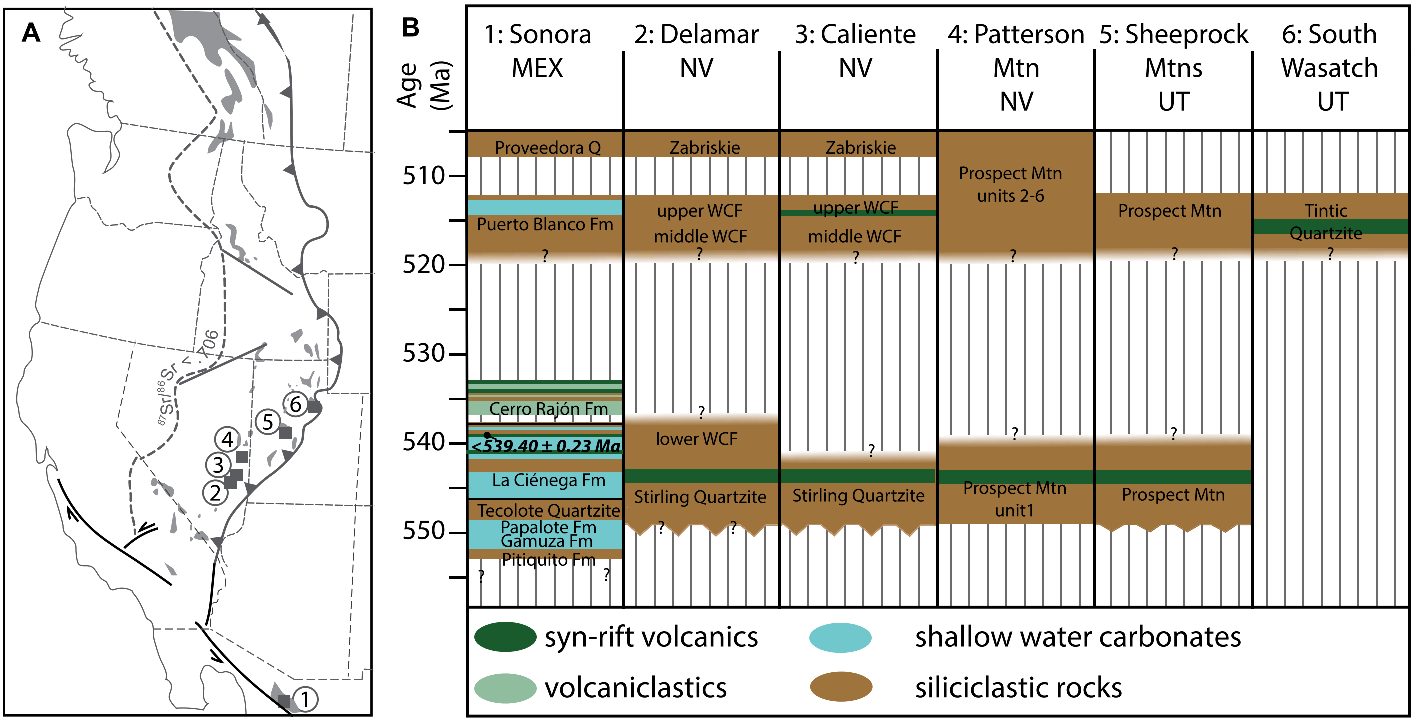

Figure 10. Localities in southwestern Laurentia with Ediacaran–Cambrian mafic volcanic units are shown. (A) Locality map for sections in Figure 10B. Grey areas show Windermere Supergroup and correlative rocks (adapted from Lund et al., 2003, 2010). (B) Localities and proposed correlations of Ediacaran–Cambrian strata in southwestern Laurentia with mafic volcanic and volcaniclastic units. The only volcanic units with radioisotopic age constraints are in Sonora, Mexico (MEX; Hodgin et al., 2021). Basalt horizons are from Stewart et al. (1984), Stewart (1970, 1972, 1974), Sorensen and Crittenden (1979), and Peterson and Clark (1974). WCF—Wood Canyon Formation; Fm—formation; NV—Nevada; UT—Utah.

Formation, and the chemistry of these units is indicative of an enriched mantle source (Barrón-Díaz et al., 2019b). Farther north in Nevada, basalt intervals occur in the latest Ediacaran–early Cambrian Stirling Quartzite and lower and upper members of the Wood Canyon Formation (Figs. 9–10; Stewart, 1970, 1974). Farther to the northeast, basalt intervals also occur within the Prospect Mountain Formation in Nevada and Utah, and the Tintic Quartzite in Utah (Stewart, 1972; Sorensen and Crittenden, 1979). The ages of these volcanic rocks and the units hosting them are not well constrained, but they are generally considered to be late Ediacaran to early Cambrian based on regional correlations (Stewart, 1972; Peterson and Clark, 1974). Given regional stratigraphic correlations, many of these basalt intervals in the southwestern United States are likely correlative with the basalts of the Cerro Rajón and La Ciénega formations in Mexico and genetically related to rift-related crustal thinning and faulting along the western and/or southern margins of Laurentia. The plumbing systems for these volcanic units have not been identified, but Ediacaran–Cambrian normal faults are plausible magmatic conduits (Fig. 8).

These volcanics are at least partially correlative to bimodal rift-related magmatism of the Wichita Province in southwestern Oklahoma that is constrained to 539.5–530 Ma (Thomas et al., 2012; Wall et al., 2021) and is thought to be part of a >250,000 km^3 large igneous province associated with rifting of the southern margin of Laurentia (Hanson et al., 2013; Brueseke et al., 2016). The Wichita volcanics also have been correlated to pulses of the Central Iapetan Magmatic Province preserved along the eastern margin of Laurentia (Youbi et al., 2020; Wall et al., 2021). Considering the unconformities that developed within the Cordilleran continental margin successions, the current exposure and distribution of volcanic rocks is likely limited by rift-related uplift and erosion. Furthermore, the original volume of rift-related basalt emplaced along the rifted margin during this interval may have been more voluminous in outboard regions (e.g., Beranek, 2017). Together, the Wichita large igneous province and the margin-wide Ediacaran–Cambrian basalts emplaced into organic-rich rift sequences could have served as a trigger for environmental and carbon-cycle change during this time.

Coincidence among a Carbon Isotope Excursion, Microbial Sedimentological Features, Biotic Turnover, and Volcanism in Western Laurentia

A coincidence of geochemical perturbations, large igneous provinces, unusual sedimentary features, and biotic turnover documented for many Phanerozoic geologic boundaries has been at the root of much speculation and debate over the cause(s) and effect(s) of coeval environmental change and mass extinction (e.g., Baud et al., 2007; Kershaw et al., 2012; Bond and Wignall, 2014). A temporal coincidence of all of these features also appears to occur across the Ediacaran–Cambrian boundary, and extinction could be mechanistically linked to the rift-related large igneous province volcanism along the margins of Laurentia—potentially partially analogous to some Phanerozoic boundaries such as the Permian–Triassic and Triassic–Jurassic.

The BACE, a large negative carbon isotope excursion in the lower Wood Canyon Formation and Esmeralda Member of the Deep Spring Formation (Corsetti and Kaufman, 1994; Corsetti and Hagadorn, 2000) is regionally reproducible

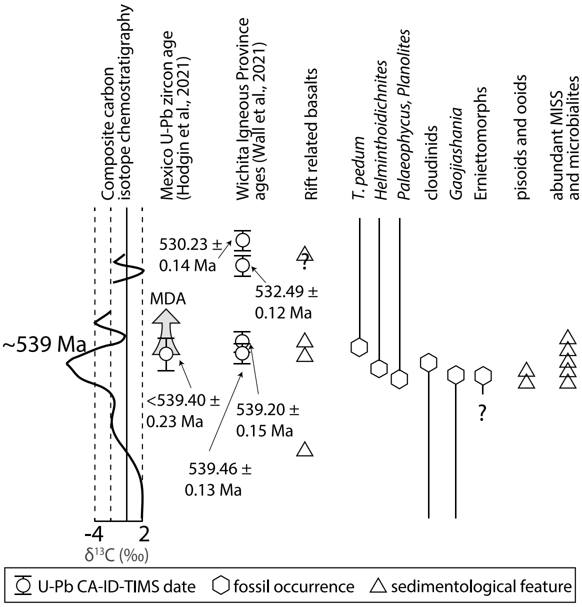

Figure 11. Diagram shows correlation of chemostratigraphy, biostratigraphy, sedimentological features, and rift-related volcanism seen across the Ediacaran–Cambrian boundary in southwestern Laurentia. U-Pb zircon ages are from Hodgin et al. (2021) and Wall et al. (2021). Trace fossil first appearances are from Corsetti and Hagadorn (2000), Jensen et al. (2002), and Waggoner and Hagadorn (2002). Last regional occurrences of Ediacaran body fossils are from Smith et al. (2016b, 2017). CA-ID-TIMS—chemical abrasion–isotope dilution–thermal ionization mass spectrometry.

across hundreds of kilometers, preserved across different shallow marine facies, different carbonate mineralogies, and multiple sequence boundaries (Fig. 7). Apart from the report of poorly preserved specimens of c.f. *Swartpuntia* from Cambrian Series 2 strata of the Poleta Formation and the upper member of the Wood Canyon Formation (Hagadorn et al., 2000), all regional occurrences of what are currently considered Ediacaran fossils are found below the BACE, and all Cambrian-type trace fossils are found above the BACE, despite the presence of similar sedimentary facies and depositional environments across the excursion (Fig. 7). Combined with consistent bio- and chemostratigraphic data from Sonora, Mexico (e.g., Hodgin et al., 2021), these data suggest that in southwestern Laurentia, the BACE coincides with biotic turnover. While some evidence for stratigraphic overlap among cloudinids and Cambrian fossil taxa has been documented in Siberia and Mongolia (Yang et al., 2016; Zhu et al., 2017), biotic turnover across the Ediacaran–Cambrian boundary is largely a globally consistent trend (e.g., Darroch et al., 2018).

A variety of microbial sedimentological features also coincide with the BACE and regional biotic turnover (Fig. 11), including stromatolites within the Esmeralda Member of the Deep Spring Formation (Fig. 4F; Oliver and Rowland, 2002), microbially induced sedimentary structures from siliciclastic strata of the Deep Spring and Wood Canyon formations (Figs. 4B and 4D; Hagadorn and Bottjer, 1997; Nelson and Smith, 2019), and pisoids, or giant ooids, from the upper Reed Dolomite and from dolomite marker beds of the lower member of the Wood Canyon Formation (Fig. 4D). Giant ooids also have been reported from the upper member of the Wood Canyon Formation (Corsetti et al., 2006). Database compilations suggest that giant ooids formed more commonly during the Neoproterozoic than during any other time in Earth history (Sumner and Grotzinger, 1993; Thorie et al., 2018), and, based on experimental and modeling work, it has been suggested that giant ooids are most likely to form under conditions in which seawater alkalinity is elevated and within seawater that is much warmer or colder than modern, low-latitude carbonate platforms (Trower et al., 2017; Trower, 2020). Although the giant ooids of the lower member of the Wood Canyon Formation are not geographically widespread, their presence, combined with regionally widespread microbial features and a large negative carbon isotope excursion, points to unusual ocean chemistry and/or climate conditions across the Ediacaran–Cambrian transition in southwestern Laurentia. A similar stratigraphic confluence of sedimentary features has been documented at other extinction boundaries, such as the end-Permian (e.g., Pruss and Bottjer, 2004; Baud et al., 2007) and the end-Triassic (e.g., Ibarra et al., 2016).

At several other major Phanerozoic geologic boundaries, age correlation between extinction events and large igneous provinces using radioisotopic dating has provided compelling evidence for mechanistic links (Wignall, 2001; Bond and Wignall, 2014), even when specific environmental and climatic changes and kill mechanism(s) resulting from individual large igneous provinces remain controversial (e.g., Bond and Wignall, 2014). If the Ediacaran–Cambrian boundary is one of the earliest extinctions of animal clades (Amthor et al., 2003; Rothman, 2017), a possible contributing trigger of this biotic turnover and the coeval BACE is the Wichita large igneous province and correlative rift-related basaltic volcanism in southwestern Laurentia (Hodgin et al., 2021). This proposed hypothesis hinges upon the demonstration of age correlation between bimodal rift volcanism within the Wichita large igneous province (Wall et al., 2021) and age constraints on carbon cycle perturbation and Ediacaran extinction, which was previously thought to have occurred at ca. 539 Ma (Linneman et al., 2019; Hodgin et al., 2021), but may have occurred at ca. 538–535 Ma (Nelson et al., 2022). While surface exposures are limited, geophysical studies and drill core data have indicated that the total volume of the volcanic body was >250,000 km^3 (Hanson et al., 2013; Hanson and Eschberger, 2014), and this is without considering the much greater potential extent of correlative, rift-related volcanic rocks around the margins of Laurentia, as discussed above. Beyond simple correlation, establishing plausible causation for the observed extinction selectivity patterns across the Ediacaran–Cambrian boundary will be equally important (Darroch et al., 2018), as will examining other geochemical evidence for environmental perturbation across this boundary.

One known problem with interpreting carbon isotope excursions that coincide with extinction horizons is that the nadirs of some of these excursions reach values below those of canonical mantle values of ~−5‰ (Javoy et al., 1986; Deines, 2002), which requires an input from another source of isotopically light carbon. For the end-Triassic, light carbon mobilized in the mantle lithosphere during the emplacement of the Central Atlantic Magmatic Province large igneous province has been hypothesized to explain the negative carbon isotope excursion (Paris et al., 2012). Others have invoked the release of light carbon during oxidation of organic-rich sediments and/or clathrate dissociation triggered by warming to explain the temporal association between volcanism and negative carbon isotope excursions (Svensen et al., 2004; Gutjahr et al., 2017; Black et al., 2018; Heimdal et al., 2020). Pulses of rift-related volcanism in southwestern Laurentia may have led to the release of light carbon through similar processes, contributing to cascading ecological and environmental changes that occurred across the Ediacaran–Cambrian boundary.

CONCLUSIONS

This study integrates new and previously published chemostratigraphic, paleontological, sedimentological, and stratigraphic data from the Death Valley region, the White-Inyo

Ranges, and Esmeralda County to explore connections between sedimentology, changes in the carbon cycle, biotic turnover, and taphonomic windows of Ediacaran organisms. Combined chemostratigraphy, lithostratigraphy, and biostratigraphy provide further, data-driven support for previous regional correlations among strata of the Ediacaran–Cambrian Death Valley region and the White-Inyo Ranges. These correlations suggest that the facies break between the regions resulted from a major late Ediacaran rift shoulder, with the Ediacaran Wyman Formation shale basin being deposited on the basinward hanging wall. The Early Permian Last Chance thrust fault may have reactivated this Ediacaran normal fault, juxtaposing the facies belts with ~30 km of shortening.

Ediacaran body fossils from the southern Great Basin and their taphonomic modes are placed within a stratigraphic framework, which shows that although their occurrences are rare, the potential for preservation of soft-bodied organisms is enhanced by the presence of clay minerals and within the base of the base of transgressive sequences. Occurrences of different taphonomic modes preserving cloudinomorphs across this Ediacaran–Cambrian sedimentary basin suggest that these organisms were living in a range of shallow marine environments with several pathways to preservation.

The BACE is a regionally reproducible carbon isotope excursion across sequence boundaries with variable sedimentary facies and variable dolomitization, which is consistent with primary derivation from changes to the isotopic composition of marine dissolved inorganic carbon and a perturbation in the global carbon cycle. This large negative carbon isotope excursion, botic turnover, and a variety of unusual, coincident sedimentological features—such as prolific stromatolites, microbial sedimentary structures, and giant ooids—coincide stratigraphically with the Ediacaran–Cambrian boundary in southwestern Laurentia. This stratigraphic boundary temporally coincides with several regionally widespread basaltic units and the Wichita large igneous province in Oklahoma, which is related to rift tectonism along the margins of Laurentia. The emplacement of volcanic magmas within newly formed, organic-rich sedimentary rift basins may have resulted in cascading environmental and ecological changes at the Ediacaran–Cambrian boundary, analogous to those at the Permian–Triassic and Triassic–Jurassic boundaries.

ACKNOWLEDGMENTS

E.F. Smith was supported by the Smithsonian Institution Peter Buck Fellowship, the Palaeontological Association Research Grant-PA-RG201703, and the American Philosophical Society Lewis and Clark Fund for Exploration and Field Research in Astrobiology. E.F. Smith is currently supported by National Science Foundation (NSF) EAR-2021064 and EAR-2144836. L.L. Nelson acknowledges the Harvard Booth Fellowship, National Geographic Early Career Grant CP-002ER-17, and NSF Graduate Research Fellowship DGE-1746891. D. Schrag, D. Fike, and D. Brenner helped support stable isotope analyses; E. Hodgin, F. Liu, and L. Webb helped with fieldwork. We thank two anonymous reviewers and associate editor G. Halverson for thoughtful and helpful comments and edits, and B. Singer for editorial assistance. We acknowledge Death Valley National Park Service, the Nevada Bureau of Land Management, and White Inyo National Forest for granting permits to E.F. Smith to conduct this research.

REFERENCES CITED

Abolins, M., Oskin, R., Prave, A.R., Summa, C., and Corsetti, F.A., 2000, Neoproterozoic glacial record in the Death Valley region, California and Nevada, *in* Lageson, D.R., Peters, S.G., and Lahren, M.M., eds., Great Basin and Sierra Nevada: Geological Society of America Field Guide 2, p. 319–335, https://doi.org/10.1130/0-8137-0002-7.319.

Ahm, A.-S.C., Maloof, A.C., Macdonald, F.A., Hoffman, P.F., Bjerrum, C.J., Bold, U., Rose, C.V., Strauss, J.V., and Higgins, J.A., 2019, An early diagenetic deglacial origin for basal Ediacaran “cap dolostones”: Earth and Planetary Science Letters, v. 506, p. 292–307, https://doi.org/10.1016/j.epsl.2018.10.046.

Ahn, S.Y., Babcock, L.E., and Hollingsworth, J.S., 2012, Revised stratigraphic nomenclature for parts of the Ediacaran–Cambrian Series 2 succession in the southern Great Basin, USA: Association of Australasian Palaeontologists Memoir 42, p. 105.

Albers, J.P., and Stewart, J.H., 1972, Geology and Mineral Deposits of Esmeralda County, Nevada: Reno, Nevada, Mackay School of Mines, University of Nevada.

Alpert, S.P., 1976, Trilobite and star-like trace fossils from the White-Inyo Mountains, California: Journal of Paleontology, v. 50, p. 226–239.

Amthor, J.E., Grotzinger, J.P., Schröder, S., Bowring, S.A., Ramezani, J., Martin, M.W., and Matter, A., 2003, Extinction of Cloudina and Namacalathus at the Precambrian–Cambrian boundary in Oman: Geology, v. 31, no. 5, p. 431–434, https://doi.org/10.1130/0091-7613(2003)031<0431:EOCANA>2.0.CO;2.

Armin, R.A., and Mayer, L., 1983, Subsidence analysis of the Cordilleran miogeocline: Implications for timing of Late Proterozoic rifting and amount of extension: Geology, v. 11, p. 702–705, https://doi.org/10.1130/0091-7613(1983)11<702:SAOTCM>2.0.CO;2.

Ball, S.H., 1907, A geologic reconnaissance in southwestern Nevada and eastern California: U.S. Geological Survey Bulletin no. 308, 221 p.

Barrón-Díaz, A.J., Paz-Moreno, F.A., and Hagadorn, J.W., 2019a, The Cerro Rajón Formation—a new lithostratigraphic unit proposed for a Cambrian (Terreneuvian) volcano-sedimentary succession from the Caborca region, northwest Mexico: Journal of South American Earth Sciences, v. 89, p. 197–210, https://doi.org/10.1016/j.jsames.2018.11.003.

Barrón-Díaz, A.J., Paz-Moreno, F.A., Lozano-Santa Cruz, R., Herrera-Urbina, S., Centeno-García, E., and López-Martínez, M., 2019b, Early Cambrian alkaline volcanism on the southern margin of Laurentia: Evidence in the volcaniclastic units from the Puerto Blanco Formation in the Caborca block, NW Mexico: International Geology Review, v. 61, no. 10, p. 1189–1206, https://doi.org/10.1080/00206814.2018.1501619.

Baud, A., Richoz, S., and Pruss, S., 2007, The lower Triassic anachronistic carbonate facies in space and time: Global and Planetary Change, v. 55, no. 1–3, p. 81–89, https://doi.org/10.1016/j.gloplacha.2006.06.008.

Beranek, L.P., 2017, A magma-poor rift model for the Cordilleran margin of western North America: Geology, v. 45, no. 12, p. 1115–1118, https://doi.org/10.1130/G39265.1.

Berner, R.A., 1990, Atmospheric carbon dioxide levels over Phanerozoic time: Science, v. 249, no. 4975, p. 1382–1386, https://doi.org/10.1126/science.249.4975.1382.

Black, B.A., Neely, R.R., Lamarque, J.-F., Elkins-Tanton, L.T., Kiehl, J.T., Shields, C.A., Mills, M.J., and Bardeen, C., 2018, Systemic swings in end-Permian climate from Siberian Traps carbon and sulfur outgassing: Nature Geoscience, v. 11, no. 12, p. 949–954, https://doi.org/10.1038/s41561-018-0261-y.

Bold, U., Ahm, A.-S.C., Schrag, D.P., Higgins, J.A., Jamsran, E., and Macdonald, F.A., 2020, Effect of dolomitization on isotopic records from Neoproterozoic carbonates in southwestern Mongolia: Precambrian Research, v. 350, https://doi.org/10.1016/j.precamres.2020.105902.

Bond, D.P., and Wignall, P.B., 2014, Large igneous provinces and mass extinctions: An update, *in* Keller, G., and Kerr, A.C., eds., Volcanism, Impacts, and Mass Extinctions: Causes and Effects: Geological Society of America Special Paper 505, p. 29–55, https://doi.org/10.1130/2014.2505(02).

Bond, G.C., and Kominz, M.A., 1984, Construction of tectonic subsidence curves for the early Paleozoic miogeocline, southern Canadian Rocky Mountains: Implications for subsidence mechanisms, age of breakup, and crustal thinning: Geological Society of America Bulletin, v. 95, no. 2, p. 155–173, https://doi.org/10.1130/0016-7606(1984)95<155:COTSCF>2.0.CO;2.

Bond, G.C., Christie-Blick, N., Kominz, M.A., and Devlin, W.J., 1985, An Early Cambrian rift to post-rift transition in the Cordillera of western North-America: Nature, v. 315, p. 742–746, https://doi.org/10.1038/315742a0.

Bouougri, E.H., Porada, H., Weber, K., and Reitner, J., 2011, Sedimentology and palaeoecology of Ernietta-bearing Ediacaran deposits in southern Namibia: Implications for infaunal vendobiont communities: Advances in Stromatolite Geobiology, v. 131, p. 473–506.

Brueseke, M.E., Hobbs, J.M., Bulen, C.L., Mertzman, S.A., Puckett, R.E., Walker, J.D., and Feldman, J., 2016, Cambrian intermediate-mafic magmatism along the Laurentian margin: Evidence for flood basalt volcanism from well cuttings in the Southern Oklahoma aulacogen (USA): Lithos, v. 260, p. 164–177, https://doi.org/10.1016/j.lithos.2016.05.016.

Burns, S.J., and Matter, A., 1993, Carbon isotopic record of the latest Proterozoic from Oman: Eclogae Geologicae Helvetiae, v. 86, no. 2, p. 595–607.

Burchfiel, B., and Davis, G.A., 1972, Structural framework and evolution of the southern part of the Cordilleran Orogen, western United States: American Journal of Science, v. 272, no. 2, p. 97–118, https://doi.org/10.2475/ajs.272.2.97.

Cai, Y., and Hua, H., 2007, Pyritization in the Gaojiashan biota: Chinese Science Bulletin, v. 52, no. 5, p. 645–650, https://doi.org/10.1007/s11434-007-0080-9.

Cai, Y., Schiffbauer, J.D., Hua, H., and Xiao, S., 2012, Preservational modes in the Ediacaran Gaojiashan Lagerstätte: Pyritization, aluminosilicification, and carbonaceous compression: Palaeogeography, Palaeoclimatology, Palaeoecology, v. 326–328, p. 109–117, https://doi.org/10.1016/j.palaeo.2012.02.009.

Catuneanu, O., 2019, Model-independent sequence stratigraphy: Earth-Science Reviews, v. 188, p. 312–388, https://doi.org/10.1016/j.earscirev.2018.09.017.

Chapman, A.D., Ernst, W., Gottlieb, E., Powerman, V., and Metzger, E.P., 2015, Detrital zircon geochronology of Neoproterozoic–Lower Cambrian passive-margin strata of the White-Inyo Range, east-central California: Implications for the Mojave–Snow Lake fault hypothesis: Geological Society of America Bulletin, v. 127, no. 7–8, p. 926–944, https://doi.org/10.1130/B31142.1.

Christie-Blick, N., and Levy, M., 1989, Stratigraphic and tectonic framework of upper Proterozoic and Cambrian rocks in the western United States, *in* Late Proterozoic and Cambrian Tectonics, Sedimentation, and Record of Metazoan Radiation in the Western United States: Pocatello, Idaho, to Reno, Nevada 20–29 July 1989, v. 331, p. 7–21.

Clapham, M.E., and Corsetti, F.A., 2005, Deep valley incision in the terminal Neoproterozoic (Ediacaran)

Johnnie Formation, eastern California, USA: Tectonically or glacially driven?: Precambrian Research, v. 141, p. 154–164, https://doi.org/10.1016/j.precamres.2005.09.002.

Cloud, P.E., and Nelson, C.A., 1966, Phanerozoic–Cryptozoic and related transitions: New evidence: Science, v. 154, no. 3750, p. 766–770, https://doi.org/10.1126/science.154.3750.766.

Coleman, D.S., Briggs, S., Glazner, A.F., and Northrup, C., 2003, Timing of plutonism and deformation in the White Mountains of eastern California: Geological Society of America Bulletin, v. 115, no. 1, p. 48–57, https://doi.org/10.1130/0016-7606(2003)115<0048:TOPADI>2.0.CO;2.

Corsetti, F.A., and Grotzinger, J.P., 2005, Origin and significance of tube structures in Neoproterozoic post-glacial cap carbonates: Example from Noonday Dolomite, Death Valley, United States: Palaios, v. 20, no. 4, p. 348–362, https://doi.org/10.2110/palo.2003.p03-96.

Corsetti, F.A., and Hagadorn, J.W., 2000, Precambrian–Cambrian transition: Death Valley, United States: Geology, v. 28, no. 4, p. 299–302, https://doi.org/10.1130/0091-7613(2000)28<299:PTDVUS>2.0.CO;2.

Corsetti, F.A. and Hagadorn, J.W., 2003, The Precambrian–Cambrian transition in the southern Great Basin, USA: The Sedimentary Record, v. 1, no. 1, p. 4–8.

Corsetti, F.A., and Kaufman, A.J., 1994, Chemostratigraphy of Neoproterozoic–Cambrian units, White-Inyo Region, eastern California and western Nevada: Implications for global correlation and faunal distribution: Palaios, v. 9, p. 211–219, https://doi.org/10.2307/3515107.

Corsetti, F.A., and Kaufman, A.J., 2003, Stratigraphic investigations of carbon isotope anomalies and Neoproterozoic ice ages in Death Valley, California: Geological Society of America Bulletin, v. 115, no. 8, p. 916–932, https://doi.org/10.1130/B25066.1.

Corsetti, F.A., Awramik, S.M., Pierce, D., and Kaufman, A.J., 2000, Using chemostratigraphy to correlate and calibrate unconformities in Neoproterozoic strata from the southern Great Basin of the United States: International Geology Review, v. 42, no. 6, p. 516–533, https://doi.org/10.1080/00206810009465096.

Corsetti, F.A., Kidder, D.L., and Marenco, P.J., 2006, Trends in oolite dolomitization across the Neoproterozoic–Cambrian boundary: A case study from Death Valley, California: Sedimentary Geology, v. 191, no. 3–4, p. 135–150, https://doi.org/10.1016/j.sedgeo.2006.03.021.

Crittenden, M.D., Jr., and Wallace, C., 1973, Possible equivalents of the Belt Supergroup in Utah, *in* Belt Symposium, Volume 1: Moscow, Idaho, Idaho Bureau of Mines and Geology, p. 116–138.

Darroch, S.A., Smith, E.F., Laflamme, M., and Erwin, D.H., 2018, Ediacaran extinction and Cambrian explosion: Trends in Ecology & Evolution, v. 33, no. 9, p. 653–663, https://doi.org/10.1016/j.tree.2018.06.003.

Darroch, S.A.F., Laflamme, M., Schiffbauer, J.D., and Briggs, D.E.G., 2012, Experimental formation of a microbial death mask: Palaios, v. 27, no. 5, p. 293–303, https://doi.org/10.2110/palo.2011.p11-059r.

DeCelles, P.G., 2004, Late Jurassic to Eocene evolution of the Cordilleran thrust belt and foreland basin system, western USA: American Journal of Science, v. 304, no. 2, p. 105–168, https://doi.org/10.2475/ajs.304.2.105.

Deines, P., 2002, The carbon isotope geochemistry of mantle xenoliths: Earth-Science Reviews, v. 58, no. 3–4, p. 247–278, https://doi.org/10.1016/S0012-8252(02)00064-8.

Diehl, P.E., 1974, Stratigraphy and sedimentology of the Wood Canyon Formation, Death Valley area, California: California Division of Mines and Geology Special Report 106, p. 37–48.

Diehl, P.E., 1979, Stratigraphy, depositional environments, and quantitative petrography of the pre-Cambrian–Cambrian Wood Canyon Formation, Death Valley [Ph.D. thesis]: University Park, Pennsylvania, Pennsylvania State University, 365 p.

Dunne, G.C., Gulliver, R.M., and Sylvester, A.G., 1978, Mesozoic evolution of rocks of the White, Inyo, Argus and Slate Ranges, eastern California, *in* Howell, D.G., and McDougall, K.A., eds., Mesozoic Paleogeography of the Western United States: Society of Economic Paleontologists and Mineralogists, Pacific Section, Book 8, p. 189–207.

Dzik, J., 1999, Organic membranous skeleton of the Precambrian metazoans from Namibia: Geology, v. 27, no. 6, p. 519–522, https://doi.org/10.1130/0091-7613(1999)027<0519:OMSOTP>2.3.CO;2.

Farmer, G.L., and Ball, T.T., 1997, Sources of Middle Proterozoic to Early Cambrian siliciclastic sedimentary rocks in the Great Basin: A Nd isotope study: Geological Society of America Bulletin, v. 109, no. 9, p. 1193–1205, https://doi.org/10.1130/0016-7606(1997)109<1193:SOMPTE>2.3.CO;2.

Fedo, C.M., and Cooper, J.D., 1990, Braided fluvial to marine transition: The basal Lower Cambrian Wood Canyon Formation, southern Marble Mountains, Mojave Desert, California: Journal of Sedimentary Petrology, v. 60, no. 2, p. 220–234.

Fedo, C.M., and Cooper, J.D., 2001, Sedimentology and sequence stratigraphy of Neoproterozoic and Cambrian units across a craton-margin hinge zone, southeastern California, and implications for the early evolution of the Cordilleran margin: Sedimentary Geology, v. 141, p. 501–522, https://doi.org/10.1016/S0037-0738(01)00088-4.

Fedo, C.M., and Prave, A.R., 1991, Extensive Cambrian braidplain sedimentation: Insights from the southwestern USA Cordillera, *in* Cooper, J.D., and Stevens, C.H., eds., Paleozoic Paleogeography of the Western United States: Society of Economic Paleontologists and Mineralogists, Pacific Section, Pacific Coast Paleogeography Symposium 1, p. 209–266.

Gehling, J.G., 1999, Microbial mats in terminal Proterozoic siliciclastics; Ediacaran death masks: Palaios, v. 14, no. 1, p. 40–57, https://doi.org/10.2307/3515360.

Gehrels, G.E., Dickinson, W.R., Ross, G.M., Stewart, J.H., and Howell, D.G., 1995, Detrital zircon reference for Cambrian to Triassic miogeoclinal strata of western North America: Geology, v. 23, no. 9, p. 831–834, https://doi.org/10.1130/0091-7613(1995)023<0831:DZRFCT>2.3.CO;2.

Germs, G., 1983, Implications of a sedimentary facies and depositional environmental analysis of the Nama Group, *in* Miller, R. McG., ed., Evolution of the Damara Orogen of South West Africa/Namibia, National Geodynamics Programme: Presenting Results of the South African Geodynamics Project on the Damara Orogen: Geological Society of South Africa Special Publication 11, p. 89–114.

Gevirtzman, D.A., and Mount, J.F., 1986, Paleoenvironments of an earliest Cambrian (Tommotian) shelly fauna in the southwestern Great Basin, USA: Journal of Sedimentary Research, v. 56, no. 3, p. 412–421.

Giallorenzo, M., Wells, M.L., Yonkee, W., Stockli, D., and Wernicke, B., 2018, Timing of exhumation, Wheeler Pass thrust sheet, southern Nevada and California: Late Jurassic to Middle Cretaceous evolution of the southern Sevier fold-and-thrust belt: Geological Society of America Bulletin, v. 130, no. 3–4, p. 558–579, https://doi.org/10.1130/B31777.1.

Gibson, B.M., Schiffbauer, J.D., and Darroch, S.A., 2018, Ediacaran-style decay experiments using mollusks and sea anemones: Palaios, v. 33, no. 5, p. 185–203, https://doi.org/10.2110/palo.2017.091.

Gibson, B.M., Rahman, I.A., Maloney, K.M., Racicot, R.A., Mocke, H., Laflamme, M., and Darroch, S.A., 2019, Gregarious suspension feeding in a modular Ediacaran organism: Science Advances, v. 5, no. 6, https://doi.org/10.1126/sciadv.aaw0260.

Gibson, B.M., Furbish, D.J., Rahman, I.A., Schmeeckle, M.W., Laflamme, M., and Darroch, S.A., 2021, Ancient life and moving fluids: Biological Reviews of the Cambridge Philosophical Society, v. 96, no. 1, p. 129–152, https://doi.org/10.1111/brv.12649.

Gilbert, G.K., 1875, Report on the Geology of Portions of Nevada, Utah, California and Arizona: Examined in the Years 1871 and 1872, *in* U.S. Army Engineer Department, Report upon Geographical and Geological Explorations and Surveys West of the One Hundredth Meridian, in Charge of First Lieut. Geo. M. Wheeler, Volume 3—Geology: Washington, D.C., U.S. Government Printing Office, p. 17–187.

Grant, S., 1990, Shell structure and distribution of Cloudina, a potential index fossil for the terminal Proterozoic: American Journal of Science, v. 290, p. 261–294.

Grazhdankin, D., 2004, Patterns of distribution in the Ediacaran Biotas: Facies versus biogeography and evolution: Paleobiology, v. 30, no. 2, p. 203–221, https://doi.org/10.1666/0094-8373(2004)030<0203:PODITE>2.0.CO;2.

Gutjahr, M., Ridgwell, A., Sexton, P.F., Anagnostou, E., Pearson, P.N., Pälike, H., Norris, R.D., Thomas, E., and Foster, G.L., 2017, Very large release of mostly volcanic carbon during the Palaeocene–Eocene Thermal Maximum: Nature, v. 548, no. 7669, p. 573–577, https://doi.org/10.1038/nature23646.

Hagadorn, J.W., and Bottjer, D.J., 1997, Wrinkle structures: Microbially mediated sedimentary structures common in subtidal siliciclastic settings at the Proterozoic–Phanerozoic transition: Geology, v. 25, no. 11, p. 1047–1050, https://doi.org/10.1130/0091-7613(1997)025<1047:WSMMSS>2.3.CO;2.

Hagadorn, J.W., and Bottjer, D.J., 1999, Restriction of a late Neoproterozoic biotope; suspect-microbial structures and trace fossils at the Vendian–Cambrian transition: PALAIOS, v. 14, no. 1, p. 73–85, https://doi.org/10.2307/3515362.

Hagadorn, J.W., and Waggoner, B., 2000, Ediacaran fossils from the southwestern Great Basin, United States: Journal of Paleontology, v. 74, p. 349–359, https://doi.org/10.1666/0022-3360(2000)0742.0.CO;2.

Hagadorn, J.W., Fedo, C.M., and Waggoner, B.M., 2000, Early Cambrian Ediacaran-type fossils from California: Journal of Paleontology, v. 74, no. 4, p. 731–740, https://doi.org/10.1666/0022-3360(2000)074<0731:ECETFF>2.0.CO;2.

Hall, J., Smith, E., Tamura, N., Fakra, S., and Bosak, T., 2020, Preservation of erniettomorph fossils in clay-rich siliciclastic deposits from the Ediacaran Wood Canyon Formation, Nevada: Interface Focus, v. 10, no. 4, https://doi.org/10.1098/rsfs.2020.0012.

Halverson, G.P., Hoffman, P.F., Schrag, D.P., Maloof, A.C., and Rice, A.H.N., 2005, Toward a Neoproterozoic composite carbon-isotope record: Geological Society of America Bulletin, v. 117, no. 9–10, p. 1181–1207, https://doi.org/10.1130/B25630.1.

Hanson, R.E., and Eschberger, A.M., 2014, An overview of the Carlton Rhyolite Group: Cambrian A-type felsic volcanism in the Southern Oklahoma Aulacogen, *in* Suneson, N.H., ed., Igneous and Tectonic History of the Southern Oklahoma Aulacogen: Oklahoma Geological Survey Guidebook 38, p. 123–142.

Hanson, R.E., Puckett, R.E., Jr., Keller, G.R., Brueseke, M.E., Bulen, C.L., Mertzman, S.A., Finegan, S.A., and McCleery, D.A., 2013, Intraplate magmatism related to opening of the southern Iapetus Ocean: Cambrian Wichita igneous province in the Southern Oklahoma rift zone: Lithos, v. 174, p. 57–70, https://doi.org/10.1016/j.lithos.2012.06.003.

Heaman, L.M., and Grotzinger, J.P., 1992, 1.08 Ga diabase sills in the Pahrump Group, California; implications for development of the Cordilleran Miogeocline: Geology, v. 20, no. 7, p. 637–640, https://doi.org/10.1130/0091-7613(1992)020<0637:GDSITP>2.3.CO;2.

Heimdal, T.H., Jones, M.T., and Svensen, H.H., 2020, Thermogenic carbon release from the Central Atlantic magmatic province caused major end-Triassic carbon cycle perturbations: Proceedings of the National Academy of Sciences of the United States of America, v. 117, no. 22, p. 11,968–11,974, https://doi.org/10.1073/pnas.2000095117.

Higgins, J.A., Blättler, C., Lundstrom, E., Santiago-Ramos, D., Akhtar, A., Ahm, A.C., Bialik, O., Holmden, C., Bradbury, H., and Murray, S., 2018, Mineralogy, early marine diagenesis, and the chemistry of shallow-water carbonate sediments: Geochimica et Cosmochimica Acta, v. 220, p. 512–534, https://doi.org/10.1016/j.gca.2017.09.046.

Hodgin, E.B., Nelson, L.L., Wall, C.J., Barrón-Díaz, A.J., Webb, L.C., Schmitz, M.D., Fike, D.A., Hagadorn, J.W., and Smith, E.F., 2021, A link between rift-related volcanism and end-Ediacaran extinction? Integrated chemostratigraphy, biostratigraphy, and U-Pb geochronology from Sonora, Mexico: Geology, v. 49, no. 2, p. 115–119, https://doi.org/10.1130/G47972.1.

Hogan, E.G., Fedo, C.M., and Cooper, J.D., 2011, Reassessment of the basal Sauk supersequence boundary across the Laurentian craton-margin hinge zone, southeastern California: The Journal of Geology, v. 119, no. 6, p. 661–685, https://doi.org/10.1086/661990.

Hollingsworth, J.S., 2011, Lithostratigraphy and biostratigraphy of Cambrian Stage 3 in western Nevada and eastern California: Museum of Northern Arizona Bulletin, v. 67, p. 26–42.

Horodyski, R., 1991, Late Proterozoic megafossils from southern Nevada: Geological Society of America Abstracts with Programs, v. 23, no. 6, p. 163.

Ibarra, Y., Corsetti, F.A., Greene, S.E., and Bottjer, D.J., 2016, A microbial carbonate response in synchrony with the end-Triassic mass extinction across the SW UK: Scientific Reports, v. 6, no. 1, p. 1–8, https://doi.org/10.1038/srep19808.

Ivantsov, A.Y., Narbonne, G.M., Trusler, P.W., Greentree, C., and Vickers-Rich, P., 2016, Elucidating Ernietta: New insights from exceptional specimens in the Ediacaran of Namibia: Lethaia, v. 49, no. 4, p. 540–554, https://doi.org/10.1111/let.12164.

Javoy, M., Pineau, F., and Delorme, H., 1986, Carbon and nitrogen isotopes in the mantle: Chemical Geology, v. 57, no. 1–2, p. 41–62, https://doi.org/10.1016/0009-2541(86)90093-8.

Jensen, S., Droser, M.L., and Heim, N.A., 2002, Trace fossils and ichnofabrics of the Lower Cambrian Wood Canyon Formation, southwest Death Valley area, *in* Corsetti, F.A., Proterozoic–Cambrian of the Great Basin and Beyond: SEPM (Society for Sedimentary Geology) Volume and Guidebook 93, p. 123–135.

Johnson, J.G., and Murphy, M.A., 1984, Time-rock model for Siluro–Devonian continental shelf, western United States: Geological Society of America Bulletin, v. 95, no. 11, p. 1349–1359, https://doi.org/10.1130/0016-7606(1984)95<1349:TMFSCS>2.0.CO;2.

Jones, D.S., Brothers, R.W., Crüger Ahm, A.-S., Slater, N., Higgins, J.A., and Fike, D.A., 2020, Sea level, carbonate mineralogy, and early diagenesis controlled $\delta^{13}C$ records in Upper Ordovician carbonates: Geology, v. 48, no. 2, p. 194–199, https://doi.org/10.1130/G46861.1.

Karlstrom, K., Hagadorn, J., Gehrels, G., Matthews, W., Schmitz, M., Madronich, L., Mulder, J., Pecha, M., Giesler, D., and Crossey, L., 2018, Cambrian Sauk transgression in the Grand Canyon region redefined by detrital zircons: Nature Geoscience, v. 11, no. 6, p. 438–443, https://doi.org/10.1038/s41561-018-0131-7.

Karlstrom, K., Mohr, M., Schmitz, M., Sundberg, F., Rowland, S., Blakey, R., Foster, J., Crossey, L., Dehler, C., and Hagadorn, J., 2020, Redefining the Tonto Group of Grand Canyon and recalibrating the Cambrian time scale: Geology, v. 48, no. 5, p. 425–430, https://doi.org/10.1130/G46755.1.

Kaufman, A.J., Corsetti, F.A., and Varni, M.A., 2007, The effect of rising atmospheric oxygen on carbon and sulfur isotope anomalies in the Neoproterozoic Johnnie Formation, Death Valley, USA: Chemical Geology, v. 237, no. 1–2, p. 47–63, https://doi.org/10.1016/j.chemgeo.2006.06.023.

Kellogg, H.E., 1963, Paleozoic stratigraphy of the southern Egan Range, Nevada: Geological Society of America Bulletin, v. 74, no. 6, p. 685–708, https://doi.org/10.1130/0016-7606(1963)74[685:PSOTSE]2.0.CO;2.

Kershaw, S., Crasquin, S., Li, Y., Collin, P.Y., Forel, M.B., Mu, X., Baud, A., Wang, Y., Xie, S., and Maurer, F., 2012, Microbialites and global environmental change across the Permian–Triassic boundary: A synthesis: Geobiology, v. 10, no. 1, p. 25–47, https://doi.org/10.1111/j.1472-4669.2011.00302.x.

Knopf, A., 1918, A Geologic Reconnaissance of the Inyo Range: And the Eastern Slope of the Southern Sierra Nevada, California: U.S. Geological Survey Professional Paper 110, 130 p.

Krogh, T., 1973, A low-contamination method for hydrothermal decomposition of zircon and extraction of U and Pb for isotopic age determinations: Geochimica et Cosmochimica Acta, v. 37, no. 3, p. 485–494, https://doi.org/10.1016/0016-7037(73)90213-5.

Kump, L.R., and Arthur, M.A., 1999, Interpreting carbon-isotope excursions: Carbonates and organic matter: Chemical Geology, v. 161, no. 1–3, p. 181–198, https://doi.org/10.1016/S0009-2541(99)00086-8.

Langille, G.B., 1974, Problematic calcareous fossils from the Stirling Quartzite, Funeral Mountains, Inyo County, California: Geological Society of America Abstracts with Programs, v. 6, p. 204–205.

Levy, M., and Christie-Blick, N., 1991, Tectonic subsidence of the early Paleozoic passive continental margin in eastern California and southern Nevada: Geological Society of America Bulletin, v. 103, no. 12, p. 1590–1606, https://doi.org/10.1130/0016-7606(1991)103<1590:TSOTEP>2.3.CO;2.

Levy, M., Christie-Blick, N., and Link, P.K., 1994, Neoproterozoic incised valleys of the eastern Great Basin, Utah and Idaho: Fluvial response to changes in depositional base level, *in* Dalrymple, R.W., Boyd, R., and Zaitlin, B.A., eds., Incised Valley Systems: Origin and Sedimentary Sequences: SEPM (Society for Sedimentary Geology) Special Publication 51, p. 369–382.

Linnemann, U., Ovtcharova, M., Schaltegger, U., Gärtner, A., Hautmann, M., Geyer, G., Vickers-Rich, P., Rich, T., Plessen, B., Hofmann, M., and Zieger, J., 2019, New high-resolution age data from the Ediacaran–Cambrian boundary indicate rapid, ecologically driven onset of the Cambrian explosion: Terra Nova, v. 31, no. 1, p. 49–58, https://doi.org/10.1111/ter.12368.

Liu, A.G., 2016, Framboidal pyrite shroud confirms the 'Death Mask' model for moldic preservation of Ediacaran soft-bodied organisms: Palaios, v. 31, no. 5, p. 259–274, https://doi.org/10.2110/palo.2015.095.

Lorentz, N.J., 2007, On protracted Laurentian rifting, continental freeboard, and cap carbonates in Neoproterozoic time [Ph.D. dissertation]: Los Angeles, University of Southern California, 168 p.

Loyd, S.J., Marenco, P.J., Hagadorn, J.W., Lyons, T.W., Kaufman, A.J., Sour-Tovar, F., and Corsetti, F.A., 2012, Sustained low marine sulfate concentrations from the Neoproterozoic to the Cambrian: Insights from carbonates of northwestern Mexico and eastern California: Earth and Planetary Science Letters, v. 339, p. 79–94, https://doi.org/10.1016/j.epsl.2012.05.032.

Ludington, S., Moring, B.C., Miller, R.J., Stone, P.A., Bookstrom, A.A., Bedford, D.R., Evans, J.G., Haxel, G.A., Nutt, C.J., and Flyn, K.S., 2007, Preliminary integrated geologic map databases for the United States: Western States: California, Nevada, Arizona, Washington, Oregon, Idaho, and Utah. Version 1: U.S. Geological Survey Open-File Report 2005-1305.

Lund, K., Aleinikoff, J.N., Evans, K.V., and Fanning, C.M., 2003, SHRIMP U-Pb geochronology of Neoproterozoic Windermere Supergroup, central Idaho: Implications for rifting of western Laurentia and synchroneity of Sturtian glacial deposits: Geological Society of America Bulletin, v. 115, no. 3, p. 349–372, https://doi.org/10.1130/0016-7606(2003)115<0349:SUPGON>2.0.CO;2.

Lund, K., Aleinikoff, J., Evans, K., DuBray, E., Dewitt, E., and Unruh, D., 2010, SHRIMP U-Pb dating of recurrent Cryogenian and Late Cambrian–Early Ordovician alkalic magmatism in central Idaho: Implications for Rodinian rift tectonics: Geological Society of America Bulletin, v. 122, no. 3–4, p. 430–453, https://doi.org/10.1130/B26565.1.

MacGabhann, B.A., Schiffbauer, J.D., Hagadorn, J.W., Van Roy, P., Lynch, E.P., Morrison, L., and Murray, J., 2019, Resolution of the earliest metazoan record: Differential taphonomy of Ediacaran and Paleozoic fossil molds and casts: Palaeogeography, Palaeoclimatology, Palaeoecology, v. 513, p. 146–165, https://doi.org/10.1016/j.palaeo.2018.11.009.

MacLean, J., Sears, J., Chamberlain, K., Khudoley, A., Prokopiev, A., Kropachev, A., and Serkina, G., 2009, Detrital Zircon Geochronologic Tests of the SE Siberia–SW Laurentia Paleocontinental Connection: Stephan Mueller Special Publication Series 4, p. 111–116, https://doi.org/10.5194/smsps-4-111-2009.

Mahon, R.C., Dehler, C.M., Link, P.K., Karlstrom, K.E., and Gehrels, G.E., 2014, Geochronologic and stratigraphic constraints on the Mesoproterozoic and Neoproterozoic Pahrump Group, Death Valley, California: A record of the assembly, stability, and breakup of Rodinia: Geological Society of America Bulletin, v. 126, no. 5–6, p. 652–664, https://doi.org/10.1130/B30956.1.

Maloney, K.M., Boag, T.H., Facciol, A.J., Gibson, B.M., Cribb, A., Koester, B.E., Kenchington, C.G., Racicot, R.A., Darroch, S.A., and Laflamme, M., 2020, Paleoenvironmental analysis of Ernietta-bearing Ediacaran deposits in southern Namibia: Palaeogeography, Palaeoclimatology, Palaeoecology, v. 556, https://doi.org/10.1016/j.palaeo.2020.109884.

Mattinson, J.M., 2005, Zircon U–Pb chemical abrasion ("CA-TIMS") method: Combined annealing and multi-step partial dissolution analysis for improved precision and accuracy of zircon ages: Chemical Geology, v. 220, no. 1–2, p. 47–66, https://doi.org/10.1016/j.chemgeo.2005.03.011.

McMahon, S., Anderson, R.P., Saupe, E.E., and Briggs, D.E., 2016, Experimental evidence that clay inhibits bacterial decomposers: Implications for preservation of organic fossils: Geology, v. 44, no. 10, p. 867–870, https://doi.org/10.1130/G38454.1.

Mehra, A., and Maloof, A., 2018, Multiscale approach reveals that Cloudina aggregates are detritus and not in situ reef constructions: Proceedings of the National Academy of Sciences, v. 115.

Miller, J.M.G., 1985, Glacial and syntectonic sedimentation: The upper Proterozoic Kingston Peak Formation, southern Panamint Range, eastern California: Geological Society of America Bulletin, v. 96, p. 1537–1553, https://doi.org/10.1130/0016-7606(1985)96<1537:GASSTU>2.0.CO;2.

Morgan, S.S., and Law, R.D., 1998, An overview of Paleozoic–Mesozoic structures developed in the central White-Inyo Range, eastern California: International Geology Review, v. 40, no. 3, p. 245–256, https://doi.org/10.1080/00206819809465208.

Morris, H.T., Lovering, T.S., and Goode, H.D., 1961, Stratigraphy of the East Tintic Mountains, Utah, with a section on Quaternary deposits: U.S. Geological Survey Professional Paper 361, 142 p.

Mount, J.F., Gevirtzman, D.A., and Signer, P.W., 1983, Precambrian–Cambrian transition problem in western North America: Part I. Tommotian fauna in the southwestern Great Basin and its implications for the base of the Cambrian System: Geology, v. 11, no. 4, p. 224–226, https://doi.org/10.1130/0091-7613(1983)11<224:PTPIWN>2.0.CO;2.

Mount, J.F., Hunt, D.L., Greene, L.R., and Dienger, J., 1991, Depositional systems, biostratigraphy and sequence stratigraphy of Lower Cambrian grand cycles, southwestern Great Basin, *in* Cooper, J.D. and Stevens, C.H., eds., Paleozoic Paleogeography of the Western United States—II: Los Angeles, California, SEPM (Society for Sedimentary Geology), Pacific Section, p. 209–226.

Naimark, E., Kalinina, M., and Boeva, N., 2018, Persistence of external anatomy of small crustaceans in a long term taphonomic experiment: PALAIOS, v. 33, no. 4, p. 154–163, https://doi.org/10.2110/palo.2017.083.

Narbonne, G.M., Myrow, P.M., Landing, E., and Anderson, M.M., 1987, A candidate stratotype for the Precambrian–Cambrian boundary, Fortune Head, Burin Peninsula, southeastern Newfoundland: Canadian Journal of Earth Sciences, v. 24, no. 7, p. 1277–1293, https://doi.org/10.1139/e87-124.

Nelson, C., 1978, Late Precambrian–Early Cambrian stratigraphic and faunal succession of eastern California and the Precambrian–Cambrian boundary: Geological Magazine, v. 115, no. 2, p. 121–126, https://doi.org/10.1017/S0016756800041169.

Nelson, C., and Durham, J.W., 1996, Guidebook for Field Trip to Precambrian–Cambrian Succession, White-Inyo Mountains, California: San Francisco, California, Geological Society of America, Paleontological Section, 17 p., https://research.nhm.org/pdfs/33847/33847-001.pdf.

Nelson, C.A., 1962, Lower Cambrian–Precambrian succession, White-Inyo Mountains, California: Geological Society of America Bulletin, v. 73, no. 1, p. 139–144, https://doi.org/10.1130/0016-7606(1962)73[139:LCSWMC]2.0.CO;2.

Nelson, C.A., 1976, Late Precambrian–Early Cambrian stratigraphic and faunal succession of eastern California and the Precambrian–Cambrian boundary: Geological Magazine, v. 115, p. 121–126, https://doi.org/10.1017/S0016756800041169.

Nelson, L.L., and Smith, E.F., 2019, Tubey or not tubey: Death beds of Ediacaran macrofossils or microbially induced sedimentary structures?: Geology, v. 47, no. 10, p. 909–913, https://doi.org/10.1130/G46473.1.

Nelson, L.L., Smith, E.F., Hodgin, E.B., Crowley, J.L., Schmitz, M.D., and Macdonald, F.A., 2020, Geochronological constraints on Neoproterozoic rifting and onset of the Marinoan glaciation from the Kingston Peak Formation in Death Valley, California (USA): Geology, v. 48, no. 11, p. 1083–1087, https://doi.org/10.1130/G47668.1.

Nelson, L.L., Ahm, A.-S.C., Macdonald, F.A., Higgins, J.A., and Smith, E.F., 2021, Fingerprinting local controls on the Neoproterozoic carbon cycle with the isotopic record of Cryogenian carbonates in the Panamint Range, California: Earth and Planetary Science Letters, v. 566, https://doi.org/10.1016/j.epsl.2021.116956.

Nelson, L.L., Ramezani, J., Almond, J.E., Darroch, S.A., Taylor, W.L., Brenner, D.C., Furey, R.P., Turner, M., and Smith, E.F., 2022, Pushing the boundary: A calibrated Ediacaran–Cambrian stratigraphic record from the Nama Group in northwestern Republic of South Africa: Earth and Planetary Science Letters, v. 580, https://doi.org/10.1016/j.epsl.2022.117396.

Newman, S.A., Daye, M., Fakra, S.C., Marcus, M.A., Pajusalu, M., Pruss, S.B., Smith, E.F., and Bosak, T., 2019, Experimental preservation of muscle tissue in quartz sand and kaolinite: PALAIOS, v. 34, no. 9, p. 437–451, https://doi.org/10.2110/palo.2019.030.

Nolan, T.B., 1924, Geology of the northwest portion of the Spring Mountains, Nevada [Ph.D. thesis]: New Haven, Connecticut, Yale University.

Nolan, T.B., 1929, Notes on the stratigraphy and structure of the northwest portion of Spring Mountain, Nevada: American Journal of Science, v. s5–17, no. 101, p. 461–472, https://doi.org/10.2475/ajs.s5-17.101.461.

Oliver, L., 1990, Stromatolites of the Lower Cambrian Deep Spring Formation; Mount Dunfee, Esmeralda County, Nevada [M.S. thesis]: Las Vegas, Nevada, University of Nevada.

Oliver, L.K., and Rowland, S.M., 2002, Microbialite reefs at the close of the Proterozoic Eon: The Middle Member Deep Spring Formation at Mt. Dunfee, Nevada, *in* Corsetti, F.A., ed., Proterozoic–Cambrian of the Great Basin and Beyond: SEPM (Society for Sedimentary Geology) Pacific Section Book 93, p. 97–122.

Paris, G., Donnadieu, Y., Beaumont, V., Fluteau, F., and Goddéris, Y., 2012, Modeling the consequences on Late Triassic environment of intense pulse-like degassing during the Central Atlantic Magmatic Province using the GEOCLIM model: Climate of the Past Discussions, v. 8, no. 3, p. 2075–2110.

Pavlis, T.L., Rutkofske, J., Guerrero, F., and Serpa, L.F., 2014, Structural overprinting of Mesozoic thrust systems in eastern California and its importance to reconstruction of Neogene extension in the southern Basin and Range: Geosphere, v. 10, no. 4, p. 732–756, https://doi.org/10.1130/GES00993.1.

Penny, A.M., Wood, R., Curtis, A., Bowyer, F., Tostevin, R., and Hoffman, K.-H., 2014, Ediacaran metazoan reefs from the Nama Group, Namibia: Science, v. 344, no. 6191, p. 1504–1506, https://doi.org/10.1126/science.1253393.

Peterson, D.O., and Clark, D.L., 1974, Trace fossils Plagiogmus and Skolithos in the Tintic Quartzite (middle Cambrian) of Utah: Journal of Paleontology, v. 48, p. 767–768.

Petrovich, R., 2001, Mechanisms of fossilization of the soft-bodied and lightly armored faunas of the Burgess Shale and of some other classical localities: American Journal of Science, v. 301, no. 8, p. 683–726, https://doi.org/10.2475/ajs.301.8.683.

Petterson, R., Prave, A.R., Wernicke, B.P., and Fallick, A.E., 2011, The Neoproterozoic Noonday Formation, Death Valley region, California: Geological Society of America Bulletin, v. 123, no. 7–8, p. 1317–1336, https://doi.org/10.1130/B30281.1.

Prave, A.R., 1999, Two diamictites, two cap carbonates, two $\delta^{13}C$ excursions, two rifts: The Neoproterozoic Kingston Peak Formation, Death Valley, California: Geology, v. 27, no. 4, p. 339–342, https://doi.org/10.1130/0091-7613(1999)027<0339:TDTCCT>2.3.CO;2.

Pruss, S.B., and Bottjer, D.J., 2004, Early Triassic trace fossils of the western United States and their implications for prolonged environmental stress from the end-Permian mass extinction: PALAIOS, v. 19, no. 6, p. 551–564, https://doi.org/10.1669/0883-1351(2004)019<0551:ETTFOT>2.0.CO;2.

Pruss, S.B., Corsetti, F.A., and Fischer, W.W., 2008, Seafloor-precipitated carbonate fans in the Neoproterozoic Rainstorm Member, Johnnie Formation, Death Valley Region, USA: Sedimentary Geology, v. 207, p. 34–40, https://doi.org/10.1016/j.sedgeo.2008.03.005.

Pu, J.P., Bowring, S.A., Ramezani, J., Myrow, P., Raub, T.D., Landing, E., Mills, A., Hodgin, E., and Macdonald, F.A., 2016, Dodging snowballs: Geochronology of the Gaskiers glaciation and the first appearance of the Ediacaran Biota: Geology, v. 44, no. 11, p. 955–958, https://doi.org/10.1130/G38284.1.

Renik, B., and Christie-Blick, N., 2013, A new hypothesis for the amount and distribution of dextral displacement along the Fish Lake Valley–northern Death Valley–Furnace Creek fault zone, California-Nevada: Tectonics, v. 32, no. 2, p. 123–145, https://doi.org/10.1029/2012TC003170.

Rooney, A.D., Austermann, J., Smith, E.F., Li, Y., Selby, D., Dehler, C.M., Schmitz, M.D., Karlstrom, K.E., and Macdonald, F.A., 2018, Coupled Re-Os and U-Pb geochronology of the Tonian Chuar Group, Grand Canyon: Geological Society of America Bulletin, v. 130, no. 7–8, p. 1085–1098, https://doi.org/10.1130/B31768.1.

Rooney, A.D., Cantine, M.D., Bergmann, K.D., Gómez-Pérez, I., Al Baloushi, B., Boag, T.H., Busch, J.F., Sperling, E.A., and Strauss, J.V., 2020, Calibrating the coevolution of Ediacaran life and environment: Proceedings of the National Academy of Sciences of the United States of America, v. 117, no. 29, p. 16,824–16,830, https://doi.org/10.1073/pnas.2002918117.

Rothman, D.H., 2017, Thresholds of catastrophe in the Earth system: Science Advances, v. 3, no. 9, https://doi.org/10.1126/sciadv.1700906.

Rowland, S.M., and Corsetti, F.A., 2002, A brief history of research on the Precambrian-Cambrian boundary in the southern Great Basin, *in* Corsetti, F.A., ed., Proterozoic-Cambrian of the Great Basin and Beyond: SEPM (Society for Sedimentary Geology), Pacific Section Book 93, p. 79-85.

Rowland, S.M., and Rodriguez, M.G., 2014, A Multicellular Alga With Exceptional Preservation From the Ediacaran of Nevada: Journal of Paleontology, v. 88, no. 2, p. 263–268, https://doi.org/10.1666/13-075.

Rowland, S.M., Oliver, L.K., and Hicks, M., 2008, Ediacaran and Early Cambrian reefs of Esmeralda County, Nevada: Non-congruent communities within congruent ecosystems across the Neoproterozoic–Paleozoic boundary, *in* Duebendorfer, E., and Smith, E., eds., Field Guide to Plutons, Volcanoes, Faults, Reefs, Dinosaurs, and Possible Glaciation in Selected Areas of Arizona, California, and Nevada: Geological Society of America Field Guide 11, p. 83–100, https://doi.org/10.1130/2008.fld011(04).

Runnegar, B., 2021, Following the logic behind biological interpretations of the Ediacaran Biotas: Geological Magazine, p. 1–25, https://doi.org/10.1017/S0016756821000443.

Schiffbauer, J.D., Selly, T., Jacquet, S.M., Merz, R.A., Nelson, L.L., Strange, M.A., Cai, Y., and Smith, E.F., 2020, Discovery of bilaterian-type through-guts in cloudinomorphs from the terminal Ediacaran Period: Nature Communications, v. 11, no. 1, p. 1–12, https://doi.org/10.1038/s41467-019-13882-z.

Seilacher, A., 1992, Vendobionta and Psammocorallia: Lost constructions of Precambrian evolution: Journal of the Geological Society, v. 149, no. 4, p. 607–613, https://doi.org/10.1144/gsjgs.149.4.0607.

Selly, T., Schiffbauer, J.D., Jacquet, S.M., Smith, E.F., Nelson, L.L., Andreasen, B.D., Huntley, J.W., Strange, M.A., O'Neil, G.R., and Thater, C.A., 2020, A new cloudinid fossil assemblage from the terminal Ediacaran of Nevada, USA: Journal of Systematic Palaeontology, v. 18, no. 4, p. 357–379, https://doi.org/10.1080/14772019.2019.1623333.

Shackleton, N., and Hall, M., 1984, Oxygen and carbon isotope data from Leg-74 foraminifers: Initial Reports of the Deep Sea Drilling Project, Volume 74: Washington, D.C., U.S. Government Printing Office, p. 599–612, https://doi.org/10.2973/dsdp.proc.74.115.1984.

Signor, P.W., and McMenamin, M.A., 1988, The Early Cambrian worm tube *Onuphionella* from California and Nevada: Journal of Paleontology, v. 62, no. 2, p. 233–240, https://doi.org/10.1017/S0022336000029863.

Signor, P.W., McMenamin, M.A., Gevirtzman, D.A., and Mount, J.F., 1983, Two new pre-trilobite faunas from western North America: Nature, v. 303, no. 5916, p. 415–418, https://doi.org/10.1038/303415a0.

Signor, P.W., Mount, J.F., and Onken, B.R., 1987, A pre-trilobite shelly fauna from the White-Inyo region of eastern California and western Nevada: Journal of Paleontology, v. 61, p. 425–438, https://doi.org/10.1017/S0022336000028614.

Slagter, S., Tarhan, L.G., Hao, W., Planavsky, N.J., and Konhauser, K.O., 2021, Experimental evidence supports early silica cementation of the Ediacara Biota: Geology, v. 49, no. 1, p. 51–55, https://doi.org/10.1130/G47919.1.

Smith, E.F., Macdonald, F.A., Crowley, J.L., Hodgin, E.B., and Schrag, D.P., 2016a, Tectonostratigraphic evolution of the c. 780–730 Ma Beck Spring Dolomite: Basin Formation in the core of Rodinia, *in* Li, Z.X., Evans, D.A.D., and Murphy, J.B., eds., Supercontinent Cycles Through Earth History: Geological Society, London, Special Publication 424, no. 1, p. 213–239, https://doi.org/10.1144/SP424.6.

Smith, E.F., Nelson, L.L., Strange, M.A., Eyster, A.E., Rowland, S.M., Schrag, D.P., and Macdonald, F.A., 2016b, The end of the Ediacaran: Two new exceptionally preserved body fossil assemblages from Mount Dunfee, Nevada, USA: Geology, v. 44, no. 11, p. 911–914, https://doi.org/10.1130/G38157.1.

Smith, E.F., Nelson, L.L., Tweedt, S.M., Zeng, H., and Workman, J.B., 2017, A cosmopolitan late Ediacaran biotic assemblage: New fossils from Nevada and Namibia support a global biostratigraphic link: Proceedings of the Royal Society B: Biological Sciences, v. 284, no. 1858, https://doi.org/10.1098/rspb.2017.0934.

Snow, J.K., and Wernicke, B.P., 2000, Cenozoic tectonism in the central Basin and Range; magnitude, rate, and distribution of upper crustal strain: American Journal of Science, v. 300, no. 9, p. 659–719, https://doi.org/10.2475/ajs.300.9.659.

Snow, J.K., Asmerom, Y., and Lux, D.R., 1991, Permian–Triassic plutonism and tectonics, Death Valley region, California and Nevada: Geology, v. 19, no. 6, p. 629–632, https://doi.org/10.1130/0091-7613(1991)019<0629:PTPATD>2.3.CO;2.

Sorensen, M.L., and Crittenden, M.D., 1979, Geologic map of the Huntsville quadrangle, Weber and Cache counties, Utah: U.S. Geological Survey Geologic Quadrangle Series Map GQ-1503, scale 1:24,000.

Spurr, J.E., 1903, Descriptive geology of Nevada south of the fortieth parallel and adjacent portions of California: U.S. Geological Survey Bulletin 208, https://doi.org/10.5962/bhl.title.46215.

Stevens, C.H., and Stone, P., 2005, Interpretation of the Last Chance thrust, Death Valley region, California, as an Early Permian décollement in a previously undeformed shale basin: Earth-Science Reviews, v. 73, no. 1–4, p. 79–101, https://doi.org/10.1016/j.earscirev.2005.04.005.

Stewart, J.H., 1965, Precambrian and Lower Cambrian formations in the Last Chance Range area, Inyo County, California: U.S. Geological Survey Bulletin 1224-A, p. A60–A70.

Stewart, J.H., 1966, Correlation of Lower Cambrian and some Precambrian strata in the southern Great Basin, California and Nevada: U.S. Geological Survey Professional Paper 550, p. C66–C72.

Stewart, J.H., 1967, Possible large right-lateral displacement along fault and shear zones in the Death Valley-Las Vegas area, California and Nevada: Geological Society of America Bulletin, v. 78, no. 2, p. 131–142, https://doi.org/10.1130/0016-7606(1967)78[131:PLRDAF]2.0.CO;2.

Stewart, J.H., 1970, Upper Precambrian and Lower Cambrian strata in the southern Great Basin, California and Nevada: U.S. Geological Survey Professional Paper 620, 206 p., https://doi.org/10.3133/pp620.

Stewart, J.H., 1972, Initial deposits in the Cordilleran geosyncline: Evidence of a late Precambrian (<850 my) continental separation: Geological Society of America Bulletin, v. 83, no. 5, p. 1345–1360, https://doi.org/10.1130/0016-7606(1972)83[1345:IDITCG]2.0.CO;2.

Stewart, J.H., 1974, Correlation of uppermost Precambrian and Lower Cambrian strata from southern to east-central Nevada: U.S. Geological Survey Journal of Research, v. 2, no. 5, p. 609–618.

Stewart, J.H., 1983, Extensional tectonics in the Death Valley area, California: Transport of the Panamint Range structural block 80 km northwestward: Geology, v. 11, no. 3, p. 153–157, https://doi.org/10.1130/0091-7613(1983)11<153:ETITDV>2.0.CO;2.

Stewart, J.H., Ross, D.C., Nelson, C., and Burchfiel, B., 1966, Last Chance thrust—A major fault in the eastern part of Inyo County, California: U.S. Geological Survey Professional Paper 550, p. D23–D34.

Stewart, J.H., Albers, J.P., and Poole, F.G., 1968, Summary of regional evidence for right-lateral displacement in the western Great Basin: Geological Society of America Bulletin, v. 79, no. 10, p. 1407–1414, https://doi.org/10.1130/0016-7606(1968)79[1407:SOREFR]2.0.CO;2.

Stewart, J.H., McMenamin, M.A., and Morales-Ramirez, J., 1984, Upper Proterozoic and Cambrian rocks in the Caborca region: Sonora, Mexico—Physical stratigraphy, biostratigraphy, paleocurrent studies, and regional relations: U.S. Geological Survey Professional Paper 1309, 36 p., https://doi.org/10.3133/pp1309.

Stockli, D.F., Dumitru, T.A., McWilliams, M.O., and Farley, K.A., 2003, Cenozoic tectonic evolution of the White Mountains, California and Nevada: Geological Society of America Bulletin, v. 115, no. 7, p. 788–816, https://doi.org/10.1130/0016-7606(2003)115<0788:CTEOTW>2.0.CO;2.

Summa, C.L., 1993, Sedimentologic, stratigraphic, and tectonic controls of a mixed carbonate-siliciclastic succession; Neoproterozoic Johnnie Formation, Southeast California [Ph.D. thesis]: Cambridge, Massachusetts, Massachusetts Institute of Technology, 615 p.

Sumner, D.Y., and Grotzinger, J.P., 1993, Numerical modeling of ooid size and the problem of Neoproterozoic giant ooids: Journal of Sedimentary Research, v. 63, no. 5, p. 974–982.

Svensen, H., Planke, S., Malthe-Sørenssen, A., Jamtveit, B., Myklebust, R., Eidem, T.R., and Rey, S.S., 2004, Release of methane from a volcanic basin as a mechanism for initial Eocene global warming: Nature, v. 429, no. 6991, p. 542–545, https://doi.org/10.1038/nature02566.

Swart, P.K., 2008, Global synchronous changes in the carbon isotopic composition of carbonate sediments unrelated to changes in the global carbon cycle: Proceedings of the National Academy of Sciences of the United States of America, v. 105, no. 37, p. 13,741–13,745, https://doi.org/10.1073/pnas.0802841105.

Swart, P.K., and Eberli, G., 2005, The nature of the $\delta^{13}C$ of periplatform sediments: Implications for stratigraphy and the global carbon cycle: Sedimentary Geology, v. 175, no. 1–4, p. 115–129, https://doi.org/10.1016/j.sedgeo.2004.12.029.

Tarhan, L.G., Hood, A.v., Droser, M.L., Gehling, J.G., and Briggs, D.E., 2016, Exceptional preservation of soft-bodied Ediacara Biota promoted by silica-rich oceans: Geology, v. 44, no. 11, p. 951–954, https://doi.org/10.1130/G38542.1.

Tarhan, L.G., Myrow, P.M., Smith, E.F., Nelson, L.L., and Sadler, P.M., 2020, Infaunal augurs of the Cambrian explosion: An Ediacaran trace fossil assemblage from Nevada, USA: Geobiology, v. 18, no. 4, p. 486–496, https://doi.org/10.1111/gbi.12387.

Taylor, M.E., 1966, Precambrian mollusc-like fossils from Inyo County, California: Science, v. 153, no. 3732, p. 198–201, https://doi.org/10.1126/science.153.3732.198.

Thomas, W.A., Tucker, R.D., Astini, R.A., and Denison, R.E., 2012, Ages of pre-rift basement and synrift rocks along the conjugate rift and transform margins of the Argentine Precordillera and Laurentia: Geosphere, v. 8, no. 6, p. 1366–1383, https://doi.org/10.1130/GES00800.1.

Thorie, A., Mukhopadhyay, A., Banerjee, T., and Mazumdar, P., 2018, Giant ooids in a Neoproterozoic carbonate shelf, Simla Group, Lesser Himalaya, India: An analogue related to Neoproterozoic glacial deposits: Marine and Petroleum Geology, v. 98, p. 582–606, https://doi.org/10.1016/j.marpetgeo.2018.08.025.

Trower, E.J., 2020, The enigma of Neoproterozoic giant ooids—Fingerprints of extreme climate?: Geophysical Research Letters, v. 47, no. 4, https://doi.org/10.1029/2019GL086146.

Trower, E.J., Lamb, M.P., and Fischer, W.W., 2017, Experimental evidence that ooid size reflects a dynamic equilibrium between rapid precipitation and abrasion rates: Earth and Planetary Science Letters, v. 468, p. 112–118, https://doi.org/10.1016/j.epsl.2017.04.004.

Turner, H., 1902, A sketch of the historical geology of Esmeralda County, Nevada: American Geologist, v. 29, p. 261–272.

Verdel, C., Wernicke, B.P., and Bowring, S.A., 2011, The Shuram and subsequent Ediacaran carbon isotope excursions from southwest Laurentia, and implications for environmental stability during the metazoan radiation: Geological Society of America Bulletin, v. 123, no. 7–8, p. 1539–1559, https://doi.org/10.1130/B30369.1.

Waggoner, B., and Hagadorn, J.W., 2002, New fossils from terminal Neoproterozoic strata of Southern Nye County, Nevada, *in* Corsetti, F.A., ed., Proterozoic–Cambrian of the Great Basin and Beyond: SEPM (Society for Sedimentary Geology) Volume and Guidebook 93, p. 87–96.

Wall, C.J., Hanson, R.E., Schmitz, M., Price, J.D., Donovan, R.N., Boro, J.R., Eschberger, A.M., and Toews, C.E., 2021, Integrating zircon trace-element geochemistry and high-precision U-Pb zircon geochronology to resolve the timing and petrogenesis of the late Ediacaran–Cambrian Wichita igneous province, Southern Oklahoma Aulacogen, USA: Geology, v. 49, no. 3, p. 268–272, https://doi.org/10.1130/G48140.1.

Wernicke, B., Axen, G.J., and Snow, J.K., 1988, Basin and Range extensional tectonics at the latitude of Las Vegas, Nevada: Geological Society of America Bulletin, v. 100, no. 11, p. 1738–1757, https://doi.org/10.1130/0016-7606(1988)100<1738:BARETA>2.3.CO;2.

Wertz, W.E., 1982, Stratigraphy and sedimentology of the Stirling Quartzite, Death Valley area, California and Nevada, *in* Cooper, J.D., Troxel, B.W., and Wright, L.A., eds., Geology of selected areas in the San Bernardino Mountains, Western Mojave Desert, and southern Great Basin, California; Geological Society of America Cordilleran Section Meeting Guidebook, Field Trip 9: Shoshone, California, Death Valley Publishing Company, p. 165–170.

Wheeler, H.E., 1948, Late pre-Cambrian–Cambrian stratigraphic cross section through southern Nevada: Nevada University Bulletin, Geology and Minerals Series 47, 58 p.

Wignall, P.B., 2001, Large igneous provinces and mass extinctions: Earth-Science Reviews, v. 53, no. 1–2, p. 1–33, https://doi.org/10.1016/S0012-8252(00)00037-4.

Wilson, L.A., and Butterfield, N.J., 2014, Sediment effects on the preservation of Burgess Shale-type compression fossils: PALAIOS, v. 29, no. 4, p. 145–154, https://doi.org/10.2110/palo.2013.075.

Witkosky, R., and Wernicke, B.P., 2018, Subsidence history of the Ediacaran Johnnie Formation and related strata of southwest Laurentia: Implications for the age and duration of the Shuram isotopic excursion and animal evolution: Geosphere, v. 14, no. 5, p. 2245–2276, https://doi.org/10.1130/GES01678.1.

Wright, L.A., Troxel, B.W., Williams, E.G., Roberts, M.T., and Diehl, P.E., 1976, Precambrian sedimentary environments of the Death Valley region, eastern California: Geologic features of Death Valley, California: California Division of Mines and Geology Special Report 106, p. 7–15.

Yang, B., Steiner, M., Zhu, M., Li, G., Liu, J., and Liu, P., 2016, Transitional Ediacaran–Cambrian small skeletal fossil assemblages from South China and Kazakhstan: Implications for chronostratigraphy and metazoan evolution: Precambrian Research, v. 285, p. 202–215, https://doi.org/10.1016/j.precamres.2016.09.016.

Yang, B., Warren, L.V., Steiner, M., Smith, E.F., and Liu, P., 2022, Taxonomic revision of Ediacaran tubular fossils: Cloudina, Sinotubulites and Conotubus: Journal of Paleontology, v. 96, no. 2, p. 256–273, https://doi.org/10.1017/jpa.2021.95.

Youbi, N., Ernst, R.E., Söderlund, U., Boumehdi, M.A., Lahna, A.A., Tassinari, C.C.G., El Moume, W., and Bensalah, M.K., 2020, The Central Iapetus magmatic province: An updated review and link with the ca. 580 Ma Gaskiers glaciation: Mass Extinctions, Volcanism, and Impacts: New Developments, v. 544, p. 35–66.

Zhu, M., Zhuravlev, A.Y., Wood, R., Zhao, F., and Sukhov, S., 2017, A deep root for the Cambrian explosion: Implications of new bio- and chemostratigraphy from the Siberian Platform: Geology, v. 45, no. 5, p. 459–462, https://doi.org/10.1130/G38865.1.

Science Editor: Brad S. Singer
Associate Editor: Galen Halverson

Manuscript Received 29 November 2021
Revised Manuscript Received 3 May 2022
Manuscript Accepted 21 June 2022

Printed in the USA